

UC Irvine

UC Irvine Previously Published Works

Title

Influence of increased isoprene emissions on regional ozone modeling

Permalink

<https://escholarship.org/uc/item/6g8188x8>

Journal

Journal of Geophysical Research Atmospheres, 103(D19)

ISSN

0148-0227

Authors

Pierce, T
Geron, C
Bender, L
[et al.](#)

Publication Date

1998-10-20

DOI

10.1029/98JD01804

Copyright Information

This work is made available under the terms of a Creative Commons Attribution License, available at <https://creativecommons.org/licenses/by/4.0/>

Peer reviewed

Influence of increased isoprene emissions on regional ozone modeling

Thomas Pierce,¹ Christopher Geron,² Lucille Bender,³
Robin Dennis,¹ Gail Tonnesen,⁴ and Alex Guenther⁵

Abstract. The role of biogenic hydrocarbons on ozone modeling has been a controversial issue since the 1970s. In recent years, changes in biogenic emission algorithms have resulted in large increases in estimated isoprene emissions. This paper describes a recent algorithm, the second generation of the Biogenic Emissions Inventory System (BEIS2). A sensitivity analysis is performed with the Regional Acid Deposition Model (RADM) to examine how increased isoprene emissions generated with BEIS2 can influence the modeling of elevated ozone concentrations and the response of ozone to changes to volatile organic compound (VOC) and nitrogen oxide (NO_x) emissions across much of eastern North America. Increased isoprene emissions are found to produce a predicted shift in elevated ozone concentrations from VOC sensitivity to NO_x sensitivity over many areas of eastern North America. Isoprene concentrations measured near Scotia, Pennsylvania, during the summer of 1988 are compared with RADM estimates of isoprene and provide support for the veracity of the higher isoprene emissions in BEIS2, which are about a factor of 5 higher than BEIS1 during warm, sunny conditions.

1. Introduction

The role of biogenic hydrocarbons on photochemical modeling has been the subject of considerable debate since the 1970s [Dimitriades and Altshuller, 1977; Lurmann *et al.*, 1984; Trainer *et al.*, 1987; Chameides *et al.*, 1988; Chock *et al.*, 1995; Simpson, 1995; Jackson *et al.*, 1996]. The National Academy of Sciences [National Research Council (NRC), 1991] emphasized the importance of including biogenic volatile organic compounds (VOCs) in ozone modeling, but recent modeling studies performed for the eastern United States [Morris *et al.*, 1997] have raised concerns about the accuracy of current biogenic emission estimates by noting gross over-predictions of isoprene concentrations when comparing model estimates with near-surface measurements of isoprene. Concern about the biogenic VOC emission inventories is understandable, because isoprene emissions from the second version of the Biogenic Emissions Inventory System (BEIS2) are about 5 times higher than those previously estimated with BEIS1 [Geron *et al.*, 1994]. Furthermore, this radical change in the magnitude of isoprene emissions may cause a shift in the simulated effectiveness of different ozone-precursor emissions abatement strategies from ones that are more effective with VOC reductions to ones that are more effective with NO_x reductions [Sillman *et al.*, 1997].

¹Air Resources Laboratory, National Oceanic and Atmospheric Administration, Research Triangle Park, North Carolina (assigned to the National Exposure Research Laboratory, U.S. EPA).

²National Risk Management Research Laboratory, U.S. Environmental Protection Agency, Research Triangle Park, North Carolina.

³DynTel Corporation, Research Triangle Park, North Carolina.

⁴National Exposure Research Laboratory, U.S. Environmental Protection Agency, Research Triangle Park, North Carolina.

⁵National Center for Atmospheric Research, Boulder, Colorado.

Copyright 1998 by the American Geophysical Union.

Paper number 98JD01804.
0148-0227/98/98JD-01804\$09.00

The purpose of this paper is three-fold: (1) to document an algorithm for estimating biogenic ozone precursor emissions for regional ozone models; (2) to examine to what extent increased isoprene emissions with this algorithm may change elevated levels of regional ozone and the sensitivity of elevated ozone to changes in VOC and NO_x anthropogenic emissions; and (3) to determine the veracity of the updated and significantly higher isoprene emissions inventory by comparing isoprene concentrations predicted with the Regional Acid Deposition Model (RADM) with measured isoprene concentrations.

2. Emissions Algorithm

The emissions algorithm developed for this study is the second version of the Biogenic Emissions Inventory System (BEIS-2). BEIS2 is an extension of the first version of BEIS [Pierce *et al.*, 1990; Pierce and Waldruff, 1991] to include a new land use inventory, updated emission factors, and revised environmental correction formulas.

BEIS2 follows the methodology recommended for the Global Emissions Inventory Activity [Guenther *et al.*, 1995]. However, BEIS2 is more advanced in that it uses more temporally resolved environmental corrections (hourly versus monthly), more spatially resolved vegetative cover (county level versus 1° latitude/longitude grid cells), and more vegetatively resolved emission factors (genus level versus broad biome classes).

2.1. Land Use

The land use database used in BEIS2 is called the Biogenic Emissions Landuse Database (BELD). Details on the development of BELD are given by Kinnee *et al.* [1997]. BELD is a melding of available land cover data sets, with an emphasis on those elements that are important for biogenic emissions calculation, namely forest and agricultural coverage. Table 1

Table 1. Hierarchy of Rules Used to Assemble the County-Level Biogenic Emissions Land use Database (BELD) Used in BEIS2

Rule Hierarchy	Description of Raw Data	Resulting BEIS2 Vegetation Classes
1	U.S. Forest Service's Eastwide Database (~1990), which contains 1-acre plot survey of ~97,000 forest locations in eastern United States. Allometric equations used diameter-at-breast-height measurements to estimate crown cover by genus.	crown cover by tree genus
2	USGS Landuse/Land Characteristics data (~1990) consisting of 1.1- km classified pixels	area of water
3	U.S. Census Bureau 1990 urbanized area boundaries	
3a	Fraction of urban area assumed to be forested [Nowak <i>et al.</i> , 1996]. Based on potential natural vegetation and relative percentages of forest/tree species in surrounding area.	urban forest/crown cover by tree genus
4	U.S. Department of Agriculture 1987 Census of Agriculture	
4a	specific crop areas	area by crop type
4b	nondesignated cropland	area assumed as misc. crop
5	USGS LULC data (see above). Land use classes (except water) assigned to land use corresponding to Guenther <i>et al.</i> [1994] emission categories. Used almost exclusively in Canada, western United States, and southern Florida.	area of generalized AVHRR classes
6	Undesignated/other. Area remaining in a county that was not allocated above.	area of other (OTHE)

Rules are followed sequentially until land use area in a county totals 100%.

lists the rules that were used to extract key features from various data sets for the BELD.

The spatial resolution of the BELD is at the county level in the United States and at the subprovince level in Canada. For air quality model applications, land use data are allocated to model grid cells using the ARC/INFO™ Geographical Information System (GIS). Table 2 shows the abundance of the most prevalent land use types estimated for the RADM domain.

2.2. Emission Factors

The emission flux factors assumed in BEIS2 are listed in Table 3 and represent leaf-on (full biomass) conditions. These fluxes have been normalized to a leaf or soil temperature of 30°C and, for isoprene, a photosynthetically active radiation (PAR) of 1000 $\mu\text{mol m}^{-2} \text{s}^{-1}$.

In Table 3, factors for tree genera have been adapted from Table 3 of Geron *et al.* [1994]. The emission factors in BEIS2, expressed as $\mu\text{g m}^{-2} \text{m}^{-1}$, were obtained from the Geron *et al.* factors (expressed as $\mu\text{g C (g foliar dry mass)}^{-1} \text{h}^{-1}$) by multiplying by the foliar density (given by Geron *et al.* as g m^{-2}) and by the compound/carbon ratio (i.e., isoprene is 68 g/60 g C). Tree genera in Geron *et al.* for which emission factors were not given, because of a lack of field measurements, have been arbitrarily assigned the lowest emission rate for each VOC category. Geron *et al.* note that these genera represent only 3.5% of forest leaf biomass in the eastern United States. An additional category, open forest (OFOR), has been added to Table 3 to account for the area in a county that is designated as forest by the U.S. Forest Service inventory statistics, but for which crown area calculations did not yield 100% coverage. The open forest category is assumed to be underbrush and is assigned a grassland emission rate for

VOC and a forest emission rate for NO. Soil NO emission factors for forests were taken from Williams *et al.* [1992].

VOC agricultural emission factors with a few exceptions are reported by Lamb *et al.* [1993] and are derived primarily

Table 2. Abundance of the Top 20 Land Use Types Found in the Biogenic Emissions Land use Database (BELD) for the RADM Domain

Land Use Type	Area, million hectares	Percent of Total
Water	318.6	36.3
Other (assumed grass)	81.6	9.3
Miscellaneous crop	75.8	8.6
Northern mixed forest	45.8	5.2
Conifer forest	39.7	4.5
Quercus (oak)	34.4	3.9
Open forest (assumed grass)	34.4	3.9
Grass	25.2	2.9
Corn	23.9	2.7
Soybeans	21.5	2.5
Woodland/cropland	21.1	2.4
Pinus (pine)	19.3	2.2
Hay	17.8	2.0
Wheat	12.8	1.5
Acer (maple)	12.1	1.4
Hardwood forest	10.6	1.2
Urban (nonforested part)	9.6	1.1
Carya (hickory)	6.6	0.8
Ulmus (elm)	4.8	0.5
Scrub	4.7	0.5
Cumulative total	820.3	93.4

The RADM modeling domain extends from (23.9°N, 98.4°W) to (49.2°N, 62.2°W), including much of eastern North America and part of the Atlantic Ocean.

Table 3. Normalized Emission Factors Assumed in the Second Version of the Biogenic Emissions Inventory System (BEIS2)

Identifier	Isoprene	Mono-terpenes	Other VOCs	NO	Description
Tree genus [Geron <i>et al.</i> , 1994]					
Abie	170	5100	2775	4.5	Abies (fir)
Acac	79.3	2380	1295	4.5	Acacia
Acer	42.5	680	693.7	4.5	Acer (maple)
Aesc	42.5	42.5	693.7	4.5	Aesculus (buck-eye)
Aila	42.5	42.5	693.7	4.5	Ailanthus
Aleu	42.5	42.5	693.7	4.5	Aleurites (tung-oil tree)
Alnu	42.5	42.5	693.7	4.5	Alnus (European alder)
Amel	42.5	42.5	693.7	4.5	Amelanchier (serviceberry)
Asim	42.5	42.5	693.7	4.5	Asimina (paw-paw)
Avic	42.5	42.5	693.7	4.5	Avicennia (black mangrove)
Betu	42.5	85	693.7	4.5	Betula (birch)
Bume	42.5	42.5	693.7	4.5	Bumelia (gum bumelia)
Carp	42.5	680	693.7	4.5	Carpinus (horn-bean)
Cary	42.5	680	693.7	4.5	Carya (hickory)
Casp	42.5	42.5	693.7	4.5	Castanopsis (chinkapin)
Cast	42.5	42.5	693.7	4.5	Castanea (chestnut)
Casu	29750	42.5	693.7	4.5	Casuarina (Austl pine)
Cata	42.5	42.5	693.7	4.5	Catalpa
Cedr	79.3	1269.3	1295	4.5	Cedrus (Deodar cedar)
Celt	42.5	85	693.7	4.5	Celtis (hack-berry)
Cerc	42.5	42.5	693.7	4.5	Cercis (redbud)
Cham	170	340	2775	4.5	Chamaecyparis (prt-orford cedar)
Citr	42.5	680	693.7	4.5	Citrus (orange)
Coru	42.5	680	693.7	4.5	Cornus (dog-wood)
Coti	42.5	42.5	693.7	4.5	Cotinus (smoke tree)
Crat	42.5	42.5	693.7	4.5	Crataegus (hawthorn)
Dios	42.5	42.5	693.7	4.5	Diospyros (persimmon)
Euca	29750	1275	693.7	4.5	Eucalyptus
Fagu	42.5	255	693.7	4.5	Fagus (american beech)
Gled	42.5	42.5	693.7	4.5	Gleditsia (honeylocust)
Gord	42.5	42.5	693.7	4.5	Gordonia (lob-lolly-bay)
Gymn	42.5	42.5	693.7	4.5	Gymnocladus (KY coffee tree)
Hale	42.5	42.5	693.7	4.5	Halesia (silver-bell)
Ilex	42.5	85	693.7	4.5	Ilex (holly)
Juni	79.3	476	1295	4.5	Juniperus (east. Red cedar)
Lagu	42.5	42.5	693.7	4.5	Laguncularia (white mangrove)
Lari	42.5	42.5	693.7	4.5	Larix (larch)
Liqu	29750	1275	693.7	4.5	Liquidambar (sweetgum)

Table 3. (continued)

Identifier	Isoprene	Mono-terpenes	Other VOCs	NO	Description
Liri	42.5	85	693.7	4.5	Liriodendron (yellow poplar)
Macl	42.5	42.5	693.7	4.5	Maclura (osage-orange)
Magn	42.5	1275	693.7	4.5	Magnolia
Malu	42.5	42.5	693.7	4.5	Malus (apple)
Meli	42.5	42.5	693.7	4.5	Melia (china-berry)
Moru	42.5	85	693.7	4.5	Morus (mulberry)
Nyss	5950	255	693.7	4.5	Nyssa (black-gum)
Ofor	56.2	140.5	84.3	4.5	Open forest (assumed grass)
Ostr	42.5	42.5	693.7	4.5	Ostrya (hophornbeam)
Oxyd	42.5	255	693.7	4.5	Oxydendrum (sourwood)
Paul	42.5	42.5	693.7	4.5	Paulownia
Pers	42.5	255	693.7	4.5	Persea (redbay)
Pice	23800	5100	2775	4.5	Picea (spruce)
Pinu	79.3	2380	1295	4.5	Pinus (pine)
Plan	42.5	42.5	693.7	4.5	Planera (water elm)
Plat	14875	42.5	693.7	4.5	Platanus (sycamore)
Popu	29750	42.5	693.7	4.5	Populus (aspen)
Pros	42.5	42.5	693.7	4.5	Prosopis (mesquite)
Prun	42.5	42.5	693.7	4.5	Prunus (cherry)
Pseu	170	2720	2775	4.5	Pseudotsuga (douglas fir)
Quer	29750	85	693.7	4.5	Quercus (oak)
Rhiz	42.5	42.5	693.7	4.5	Rhizophora (red mangrove)
Sabl	5950	42.5	693.7	4.5	Sabal (cabbage palmetto)
Sali	14875	42.5	693.7	4.5	Salix (willow)
Sapi	42.5	42.5	693.7	4.5	Sapium (chinese tallow tree)
Sass	42.5	42.5	693.7	4.5	Sassafras
Sere	14875	42.5	693.7	4.5	Serenoa (saw palmetto)
Sorb	42.5	42.5	693.7	4.5	Sorbus (mountain ash)
Swie	42.5	42.5	693.7	4.5	Swietenia (W. Indies mahogany)
Taxo	42.5	1275	693.7	4.5	Taxodium (cypress)
Thuj	170	1020	2775	4.5	Thuja (W. red cedar)
Tili	42.5	42.5	693.7	4.5	Tilia (basswood)
Tsug	79.3	158.7	1295	4.5	Tsuga (Eastern hemlock)
Ulmu	42.5	42.5	693.7	4.5	Ulmus (American elm)
Vacc	42.5	42.5	693.7	4.5	Vaccinium (blueberry)
Wash	5950	42.5	693.7	4.5	Washingtonia (fan palm)
Agriculture					
Alfa	19	7.6	11.4	12.8	Alfalfa
Barl	7.6	19	11.4	256.7	Barley
Corn	0.5	0	0	577.6	Corn
Cott	7.6	19	11.4	256.7	Cotton
Hay	37.8	94.5	56.7	12.8	Hay
Mscp	7.6	19	11.4	12.8	Misc crops
Oats	7.6	19	11.4	256.7	Oats
Past	56.2	140.5	84.3	57.8	Pasture

Table 3. (continued)

Identifier	Isoprene	Mono-terpenes	Other VOCs	NO	Description
Pean	102	255	153	12.8	Peanuts
Pota	9.6	24	14.4	192.5	Potato
Rice	102	255	153	0.2	Rice
Rye	7.6	19	11.4	12.8	Rye
Sorg	7.8	19.5	11.7	577.6	Sorghum
Soyb	22	0	0	12.8	Soybean
Toba	0	58.8	235.2	256.7	Tobacco
Whea	15	6	9	192.5	Wheat
USGS land cover/Guenther et al. [1994] factors					
Borf	910	713	755	4.5	Boreal forest
Conf	1550	1564	1036	4.5	Conifer forest
Cswt	1050	660	770	0.2	Herbaceous wetlands
Desh	65	94.5	56.7	57.8	Desert shrub
Harf	8730	436	882	4.5	Hardwood forest
Mixf	11450	1134	1140	4.5	Mixed forest
Nmxf	10150	1100	850	4.5	Northern mixed forest
Oksv	7350	100	600	4.5	Oak savanna
Pacp	55	79.8	47.9	35.3	Pasture cropland
Scwd	2700	349	651	31.2	Scrub woodland
Shrf	10750	530	910	4.5	SE/W deciduous forest
Smxf	17000	1500	1250	4.5	Southeast mixed forest
Spin	1460	1983	1252	4.5	Southern pine
Wcnf	4270	1120	1320	4.5	Western coniferous forest
Wdcp	2550	663	2053	8.7	Woodland/cropland
Wetf	3820	923	1232	0.2	Wetland forest
Wmxf	5720	620	530	4.5	Western mixed forest
Wwdl	525	250	360	4.5	Western woodlands
Miscellaneous					
Barr	0	0	0	0	Barren
Cnif	745.4	1366.6	993.9	4.5	Conifer forest (BEIS1 only)
Gras	56.2	140.5	84.3	57.8	Grass
Oak	3108.3	255.5	894.2	4.5	Oak forest (BEIS1 only)
Oacd	2112.4	368.8	871.8	4.5	Other deciduous (BEIS1 only)
Othe	56.2	140.5	84.3	57.8	Other (assumed grass)
Rang	37.8	94.5	56.7	57.8	Range
Scru	37.8	94.5	56.7	57.8	Scrub
Snow	0	0	0	0	Snow
Tund	2411.7	120.6	150.7	0.2	Tundra (Guenther et al., 1995)
Ufor	1988.7	663.7	920	4.5	Urban forest (BEIS1 only)
Ugra	56.2	140.5	84.3	57.8	Urban grass (BEIS1 only)
Uoth	11.2	28.1	16.9	11.6	Urban other (20% grass)
Urba	408.6	161.9	200.5	12.5	Urban (BEIS1 only)
Utre	5140	1000	959	4.5	Urban trees (.5 Harf/.5 Conf)
Wate	0	0	0	0	Water

Emission factors are expressed in terms of $\mu\text{g m}^{-2} \text{h}^{-1}$ and are normalized to 30°C. Isoprene emissions are also normalized to a photosynthetically active radiation value of $1000 \mu\text{mol m}^{-2} \text{s}^{-1}$.

from measurements taken during the 1970s. The significantly lower emission factor for corn (compared to BEIS1) is based on work by *Sharkey et al.* [1992]. For miscellaneous crops, a nominal VOC emission factor has been assumed. Agricultural lands represent most of the soil NO in the BEIS2 algorithm. These flux factors are based on *Williams et al.* [1992], and the emission rates for crops are sorted by nitrogen fertilizer application rates. Because rice is grown in a wet environment, the wetlands emission rate is assumed for NO.

The USGS land use data are used mostly in Canada and in portions of the western United States, where genus-level forest cover and agricultural crop data were unavailable. The VOC emission fluxes proposed by *Guenther et al.* [1994] were assigned to our synthesis of the USGS database to arrive at 18 land use/emission factor classes. The most prevalent USGS classes in the RADM domain are northern mixed forest (NMXF, 5%), conifer forest (CONF, 5%), woodland/cropland (WDCP, 2%), and hardwood forest (HARF, 1%). The VOC emission factors for NMXF are an area-weighted average of the three northern mixed forest classes from Table 4 of *Guenther et al.*, except that the branch shading effect has been removed by multiplying the isoprene emission factor by 1.75 (as suggested by *Guenther et al.*). In BEIS2, canopy shading is accounted for in the environmental correction algorithm (discussed below in section 2.3). VOC emission factors for CONF and HARF are taken from Table 5 of *Guenther et al.* and are also adjusted for shading effects. VOC factors for WDCP are taken from Table 5 of *Guenther et al.*, except no shading effects are assumed. Soil NO emission factors are based on the forest emission rate from *Williams et al.* [1992], except that the WDCP factor is split equally between forest and miscellaneous crops.

Several of the miscellaneous emission factors listed in Table 3 are included for historical or testing purposes as they are vestiges from the BEIS1 model. Miscellaneous factors that warrant mention because of their use in BEIS2 include barren (BARR), grass (GRAS), other (OTHE), scrub (SCRU), tundra (TUND), urban other (UOTH), urban trees (UTRE), and water (WATE). Emissions from barren and water are assumed to be zero. The other category (OTHE), which represents areas of the domain that could not be classified, is arbitrarily assumed to consist of grassland. The isoprene factor for OTHE may underestimate isoprene emissions because forested areas are not included. Grassland and scrub emission factors are taken from BEIS1 [*Pierce and Waldruff*, 1991]. The tundra category, although not part of this RADM domain, is taken from a global data base prepared by *Guenther et al.* [1995].

Special treatment has been given to urbanized areas. Atlases of potential vegetation were consulted to determine whether the potential natural vegetation for an urban area is either forest or grassland. Then based on work of *Nowak et al.* [1996], urban areas are assumed to consist of either 32% tree cover (forested regions), 22% tree cover (grassland regions), or 11% tree cover (desert regions, not applicable in this modeling domain). In the eastern United States, where forest inventory data were available, tree genus distributions are taken from nearby county inventory statistics. Urban forest areas outside of the eastern United States are assigned to the urban tree (UTRE) category, which is simply assumed to consist of 50% hardwood forests (HARF) and 50% coniferous forests (CONF). The remainder of the urban area (UOTH) is assumed to consist of 20% grass and 80% barren.

2.3. Environmental Corrections

Environmental correction algorithms for biogenic VOCs are based on the work of *Guenther et al.* [1994] and *Geron et al.* [1994] and for soil NO are based on *Williams et al.* [1992]. Isoprene emissions, which are assumed to vary as a function of leaf temperature and visible solar radiation, are computed as follows:

$$I = I_s \times C_L \times C_T \quad (1)$$

where I is the adjusted isoprene emissions flux, and I_s is the isoprene emissions flux standardized to a leaf temperature T of 30°C and a photosynthetically active radiation (PAR) of 1000 $\mu\text{mol m}^{-2} \text{s}^{-1}$. The light adjustment factor C_L is estimated as follows:

$$C_L = \frac{\alpha_{L1} \text{PAR}}{\sqrt{1 + \alpha^2 \text{PAR}^2}} \quad (2)$$

where α (=0.0027) and c_{L1} (=1.066) are empirically derived coefficients. The leaf temperature adjustment factor C_T , which was also derived empirically from laboratory data, is computed as follows:

$$C_T = \frac{\exp[c_{T1}(T - T_s)/RT_sT]}{1 + \exp[c_{T2}(T - T_m)/RT_sT]} \quad (3)$$

where c_{T1} equals 95,000 J mol^{-1} , T_s is the standardized temperature (303 K), R is the ideal gas constant (8.314 $\text{K}^{-1} \text{mol}^{-1}$), c_{T2} equals 230,000 J mol^{-1} , and T_m equals 314 K. PAR is computed as a function of height at five levels via the following:

$$\text{PAR}_z = \text{PAR}_0 \times \exp[-0.42 \times \text{LAI}_z] \quad (4)$$

where PAR_z is computed as a function of height z , PAR_0 is estimated for the top of the canopy, and LAI_z is the leaf area index summed from the top of the canopy ($z=0$) down to height z . Total LAI is assumed to be 3 ($\text{m}^2 \text{m}^{-2}$) for pines, 5 for deciduous trees, and 7 for other coniferous genus types.

In BEIS2, leaf temperature is assumed simply to equal ambient temperature, because of the difficulties in establishing a reliable leaf energy balance model [*Fuentes et al.*, 1995; *Lamb et al.*, 1996]. Sensitivity studies of *Lamb et al.* [1993] showed that ignoring the difference in leaf temperature relative to ambient temperature can change biogenic VOC emission fluxes by -33 to +50%. Future versions of BEIS will include a more robust canopy model, when the leaf energy balance algorithm has been improved.

Leaf biomass is distributed uniformly with height, except for deciduous trees where the specific leaf weight is assumed to vary as a function of height, so that the distribution of leaf biomass varies from top to bottom (27, 21, 18, 17, and 17%) according to *Geron et al.* [1994]. This adjustment increases isoprene emissions from deciduous genus types by as much as 10% because light levels are higher in the upper portions of the canopy.

Emissions for other biogenic VOCs, E , are assumed to vary only as a function of leaf temperature as follows:

$$E = E_s \times \exp[0.09(T - T_s)] \quad (5)$$

where E_s is the standardized emissions flux for monoterpenes and other VOCs, T is the leaf temperature (K), and T_s is the

standardized temperature (30°C). For soil NO emissions, the equations of *Williams et al.* [1992] are restructured in a similar manner as the biogenic VOC correction equations as follows:

$$\text{NO} = \text{NO}_0 \times \exp[0.071(T - T_s)] \quad (6)$$

where NO is the adjusted soil NO emissions flux, NO_0 is the emissions flux standardized to a soil temperature T_s of 30°C, and T is the soil temperature. Soil temperature is based on minor adjustments of the ambient air temperature using empirical relationships given by *Williams et al.* [1992].

2.4. Differences in BEIS1 and BEIS2

In this paper, we assume that isoprene emissions from BEIS2 are a factor of 5 higher than BEIS1. The increase in isoprene arising from the BEIS2 algorithm is caused mostly by changes in the base emission factors assumed for trees and may be attributed to several interrelated causes. The BEIS1 isoprene factors were based mostly on branch enclosure measurements collected near Tampa Bay, Florida, in the mid-1970s [*Zimmerman*, 1979]. At the time, these measurements were assumed to represent fully illuminated conditions, as solar radiation measurements were unavailable. However, *Lamb et al.* [1993] reasoned that these measurements in most instances were partially shaded, so that isoprene emission factors derived from the Tampa Bay study for isoprene should be increased by about a factor of 2. *Guenther et al.* [1994] similarly note that branch shading effects may cause emission factors derived from leaf cuvette measurements (which are used in most modern field measurements) to be about a factor of 1.75 higher than emission factors derived from branch enclosures. *Lamb et al.* [1993] note that the BEIS1 isoprene factors were based on geometric means, which represent the central tendency of a skewed set of measurements. However, factors from *Geron et al.* [1994] and *Guenther et al.* [1994], assumed in BEIS2, are based on arithmetic means, which represent the mean mass flux. Use of arithmetic means increases isoprene emission factors by about a factor of 2. The relative merits of geometric means versus arithmetic means are discussed by *Lamb et al.* [1993, p. 1676]. The combined effect of these causes is difficult to compute exactly because the BEIS2 algorithm also includes new emission measurements that allow the emission factors to be estimated for 76 tree genera while BEIS1 contains emission factors for only 3 broad forest types. Nevertheless, calculations performed by *Geron et al.* [1995] for the Atlanta, Georgia, area indicate that daily isoprene emissions with BEIS2 were about a factor of 5 higher than BEIS1. Therefore, in the modeling performed for this paper, we assume simply a factor of 5 difference in isoprene emissions to allow for a systematic comparison of BEIS1-equivalent emissions and BEIS2.

3. Ozone Model Sensitivity

The sensitivity of RADM to changes in biogenic VOC emissions is examined for the period July 28 to August 6, 1988. This period had two pulses of relatively high regional ozone levels in the eastern United States. Further details on the meteorology and air quality patterns during this period are given by *Dennis et al.* [1990].

Table 4. Most Prevalent Land Use Categories Used in Computing Biogenic Emissions for the 80 km x 80 km RADM Grid Cell Overlaying Scotia, Pennsylvania

Vegetation Type	Percent of Total Grid
Forest categories (73%)	
Quercus (oak)	33
Acer (maple)	10
Open forest (assumed grass)	5
Betula (birch)	3
Carya (hickory)	2
Pinus (pine)	2
Sassafras	2
Prunus (cherry)	2
Agricultural categories (17%)	
Hay	6
Corn	5
Miscellaneous crop	4
Miscellaneous categories (10%)	
Other (assumed grass)	9
Urban (includes forest)	1

Only those forest and agricultural categories comprising at least 2% of the grid are listed.

3.1. Modeling Assumptions

Simulations from version 2 of the Regional Acid Deposition Model (RADM) [Chang *et al.*, 1987] are used to examine ozone sensitivity and in section 4 to compare against measured isoprene concentrations. For this study, we have employed a 21-layer version of RADM, consisting of 35 x 38 grid cells each having a horizontal resolution of 80 km. The modeling domain extends from (23.9° N, 98.4° W) to (49.2° N, 62.2° W). Because of computational restraints, horizontal grid resolution in the model has been sacrificed to allow more detailed simulation of vertical processes, which are believed to be important for isoprene distributions. Near the surface, modeled layer depths are ~40 m. The relatively coarse 80-km grid resolution is deemed adequate for examining isoprene at Scotia, Pennsylvania, because the land use around this site is similar to that for the corresponding model grid cell as listed in Table 4. An 80-km grid is also probably adequate for examining regional ozone, as a sensitivity analysis performed using RADM with a 20-km and an 80-km grid resolution for the northeastern United States showed very similar percentage changes in regional ozone due to emission changes. We are, however, less confident about using the coarse grid cell reso-

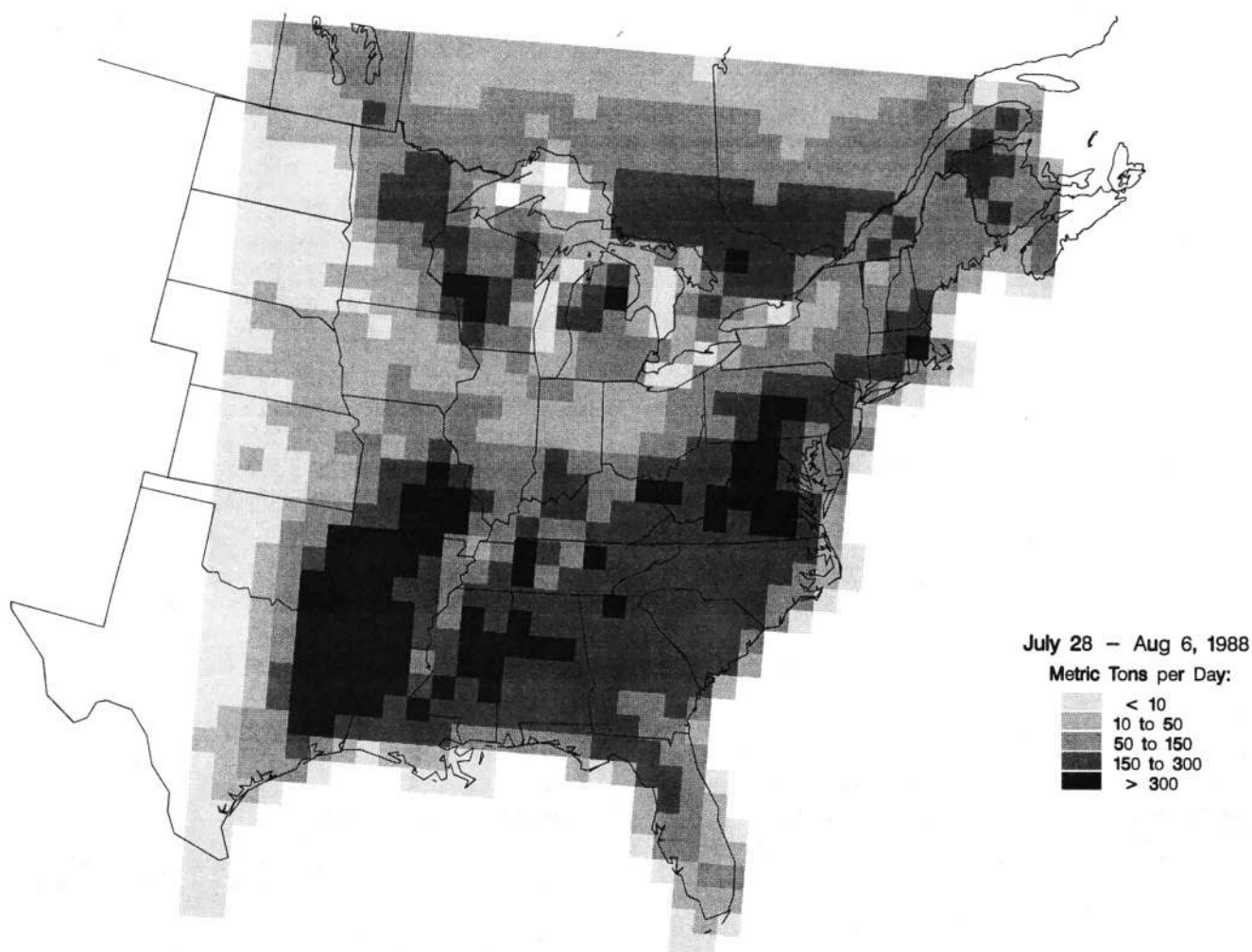


Figure 1. Mean daily isoprene emissions estimated with BEIS2 averaged over the period July 28 to August 6, 1988. Grid cells are approximately 80 km x 80 km in size.

lution in RADM to examine ozone sensitivity for urban areas, and the sensitivity of modeled ozone reported here should be viewed from a regional, nonurban perspective.

RADM handles numerous physical and chemical processes, including advection, vertical diffusion, cloud effects on vertical transport and actinic flux, dry and wet deposition, and gas and aqueous chemistry. Vertical eddy diffusivity is treated using first-order similarity theory equations, as described by Byun and Dennis [1995]. Boundary layer calculations needed for determining vertical eddy diffusivity and dry deposition are taken from the fifth-generation Penn State/NCAR mesoscale meteorological model (MM5) [Grell *et al.*, 1994]. Dry deposition processing in RADM follows Wesely [1989], although VOC species such as isoprene are not deposited in the model because of a lack of experimental data. RADM uses the RADM2 chemical mechanism developed by Stockwell *et al.* [1990]. For this paper, model simulations are available for the period July 19 to August 26, 1988.

Anthropogenic emissions are taken from the 1990 interim inventory [U.S. EPA, 1993]. As discussed earlier, biogenic emissions estimates for the so-called BEIS1-equivalent data set is simply obtained by taking the BEIS2 inventory and dividing the isoprene emissions by a factor of 5, which is con-

sistent with Geron *et al.* [1995]. BEIS2 has been adapted for use with the RADM by using the ARC/INFO™ Geographical Information System (GIS) to project the land use from the BELD onto the 80-km x 80-km grids. Near-surface temperature and solar radiation values as calculated by MM5 are used to compute gridded biogenic emissions on an hourly basis. Gridded patterns of daily isoprene, total biogenic VOC, and biogenic NO emissions averaged over the period July 28 to August 6, 1988, are shown in Figures 1-3. Isoprene and VOC patterns align closely with land use patterns, with the highest fluxes occurring in mixed oak forests near the Appalachian and Ozark Mountains. Biogenic NO emissions correspond to agricultural regions and are highest in the "corn belt" of the midwestern United States. Biogenic emissions follow a distinct diurnal pattern, as they are influenced by temperature and, for isoprene, sunlight. Day-to-day changes in biogenic emissions are influenced by variability in synoptic weather patterns, with clear warm conditions bringing higher VOC and NO emissions.

3.2. RADM Results

For this sensitivity analysis, nine model simulations have been performed. Superimposed on the three base case sce-

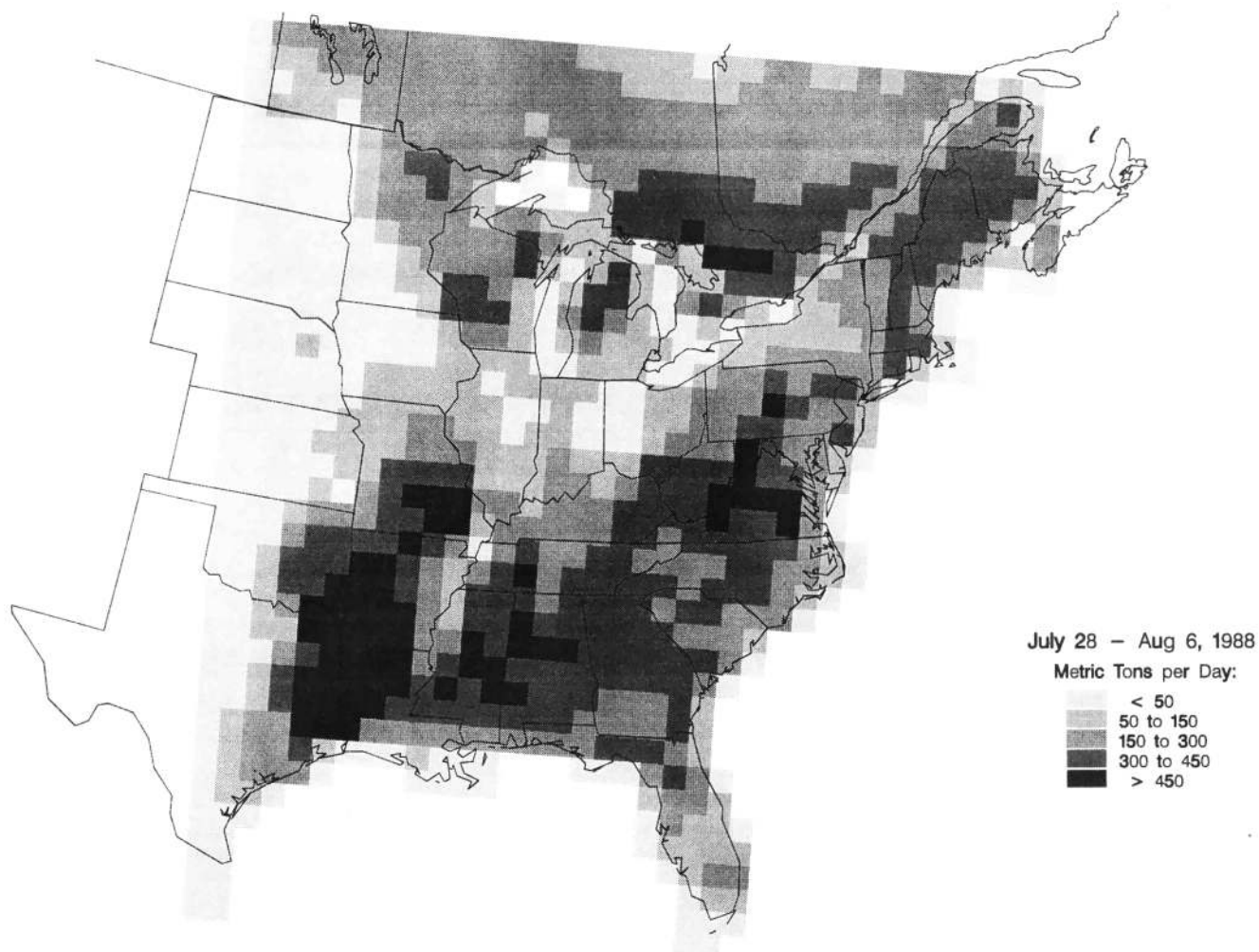


Figure 2. Mean daily total biogenic VOC emissions estimated with BEIS2 averaged over the period July 28 to August 6, 1988.

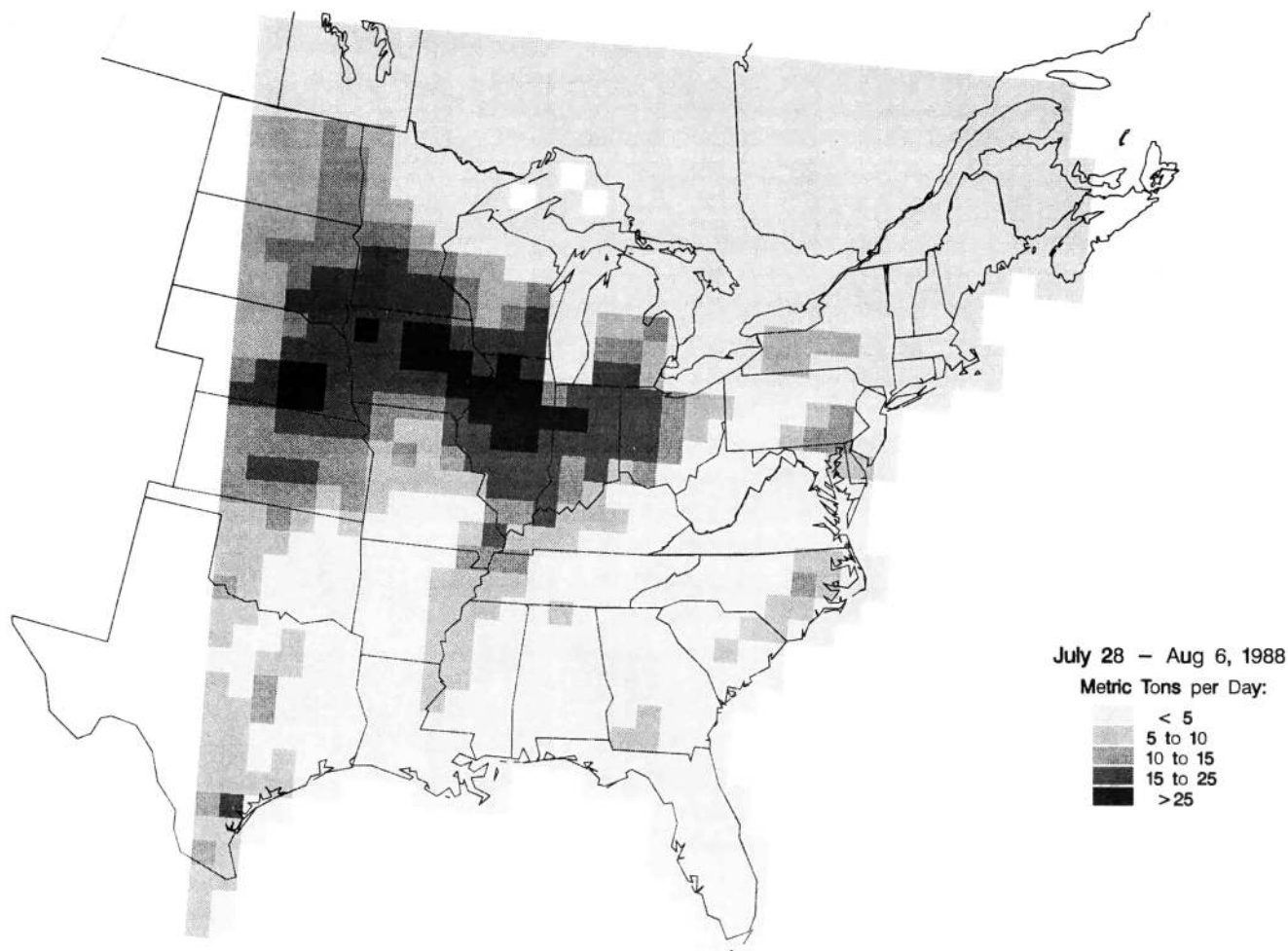


Figure 3. Mean daily biogenic NO emissions estimated with BEIS2 averaged over the period July 28 to August 6, 1988. Emissions are expressed as NO, not as NO₂.

narios (no biogenic emissions, BEIS1-equivalent emissions, BEIS2 emissions) are simulations with a 50% reduction in anthropogenic VOC emissions and simulations with a 50% reduction in anthropogenic NO_x emissions.

Maps showing peak ozone estimates for the three “base case” scenarios are given in Figure 4. The no-biogenic emissions scenario (Figure 4a) results in a relatively small area of elevated (>90 ppb) ozone concentrations. Ozone levels >120 ppb are modeled along the Northeast coast, over portions of the Great Lakes, and near the border of Texas and Louisiana. The area of elevated ozone expands with the addition of BEIS1-equivalent emissions (Figure 4b), with levels >90 ppb common across much of the eastern United States. With BEIS2 (Figure 4c), the area of elevated ozone levels expands even farther. Peak concentrations >120 ppb stretch from St. Louis to southern Ontario and from North Carolina to northern Maine. Other pockets of ozone >120 ppb are modeled in the upper South and along the Gulf Coast.

The effect of biogenic emissions estimates on VOC versus NO_x emissions sensitivity can be seen in the percentage change maps given in Figure 5. Percentage change has been computed relative to the three base case simulations shown in Figure 4. For the no-biogenic (anthropogenic only) scenario, 50% VOC emission reductions result in lowered peak ozone

(Figure 5a), especially around the Great Lakes and along the Northeast Corridor. Figure 5b shows that reductions in NO_x emissions caused ozone reductions across most of the domain, but for several cells with strong urban or power plant NO_x sources, the NO_x emission reduction caused an increase in ozone. Reducing VOC emissions with the BEIS1-equivalent scenario (Figure 5c) shows only a modest reduction in the number of grid cells with elevated ozone, but peak concentrations near New York City, Lake Erie, and near Houston are notably reduced. NO_x emission reductions (Figure 5d) result in widespread decreases away from urban areas, but high levels persist near New York City and Chicago. Only three cells show an ozone increase with NO_x reduction compared with nine cells in Figure 5b. For the BEIS2 emissions scenario, reducing VOC emissions by 50% (Figure 5e) results in little overall effect on peak ozone across much of the modeling domain, but ozone near the major NO_x emission source regions of New York City and Chicago show some decreases. Decreases in peak ozone are seen across most of the domain with a 50% NO_x emissions reduction (Figure 5f).

The peak ozone maps and the changes in peak ozone shown in Figures 4 and 5 provide a qualitative basis for comparing peak ozone, but more robust measures of regional model sensitivity can be obtained by looking at nonurban grid

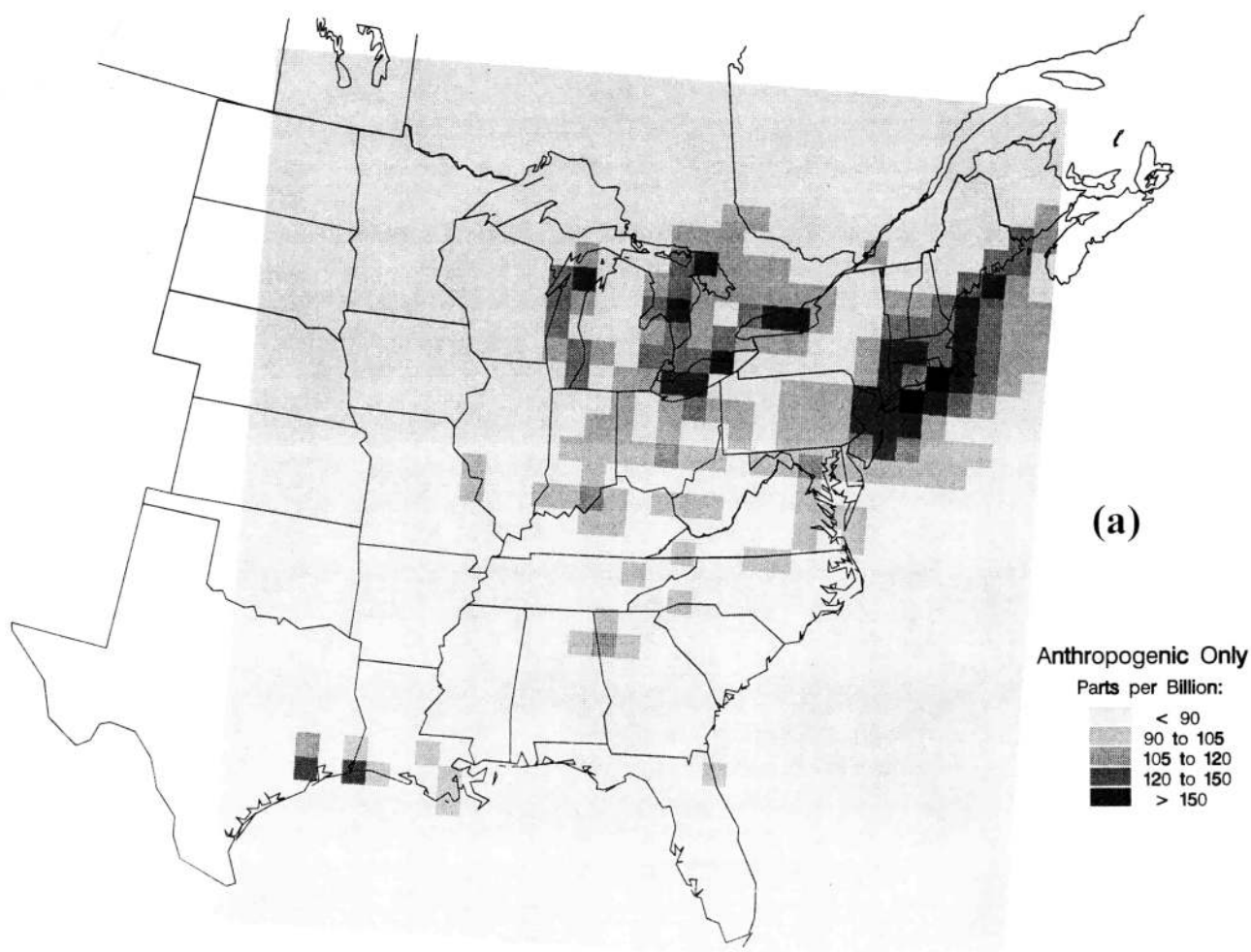


Figure 4. Maximum hourly ozone predicted at each RADM grid cell for the period July 28 to August 6, 1988. (a) No biogenic emissions, (b) BEIS1-equivalent biogenic emissions, and (c) BEIS2 biogenic emissions.

cells for several additional ozone metrics: number of grid cell hours >80 ppb, number of grid cell hours >120 ppb, and the number of grid cell hours >150 ppb. Twenty-two urban grid cells have been excluded from further sensitivity analysis because the relatively coarse grid resolution (80 km) makes it difficult to draw conclusions about urban O_3 sensitivity. Values for the three ozone metrics are shown for all nine model simulations in Table 5. For all metrics, it is readily apparent that changes in biogenic emissions influence elevated levels of regional ozone, with higher biogenic emissions generally resulting in higher ozone levels.

While the ozone metrics show sensitivity to biogenic emissions for the base case emission scenarios, perhaps of greater interest is the relative sensitivity of elevated ozone levels to biogenic emissions as a function of VOC versus NO_x emissions reductions. To examine this, we define a relative VOC/ NO_x effectiveness index (REI) as follows:

$$REI = \frac{\text{metric}_{50\%NO_x} - \text{metric}_{50\%VOC}}{\text{metric}_{base}} \quad (7)$$

where the metrics are taken from Table 5 for the 50% NO_x , 50% VOC, and base emissions scenarios. REIs for each metric and biogenic emissions scenario are listed in Table 6. As

an example, using the number of grid cell hours >80 ppb metric, the REI for “no BEIS” scenario is calculated to be +0.1%. This value is calculated from data in Table 5 as $(2380 - 2371)/6326$, and then multiplied by 100. The value of +0.1% implies that the VOC emission reduction scenario is +0.1% more effective than the NO_x emission reduction scenario in reducing the number of grid cell hours >80 ppb for the “no BEIS” emissions base case. Table 6 is arranged so that biogenic emissions increase from left to right, and more stringent ozone metrics increase from top to bottom. As might be expected, ozone metrics are more NO_x sensitive (have more negative REI scores) with higher biogenic VOC emissions and lower ozone levels. Simulations with BEIS2 favor NO_x emission reductions for all ozone metrics, whereas simulations with no biogenic emissions (no BEIS) favor VOC emission reductions for all ozone metrics. Table 6 indicates a shift from VOC emission effectiveness (reflected in positive REI values) to NO_x emission effectiveness (reflected in negative REI values). The >80 ppb metric shows that both BEIS1 and BEIS2 emissions favor NO_x emissions reductions. For the >120 ppb metric, REIs show a switch from VOC effective to NO_x effective in moving from BEIS1 to BEIS2.

These sensitivity results indicate why there is so much interest in biogenic emissions. First, the predicted ozone levels

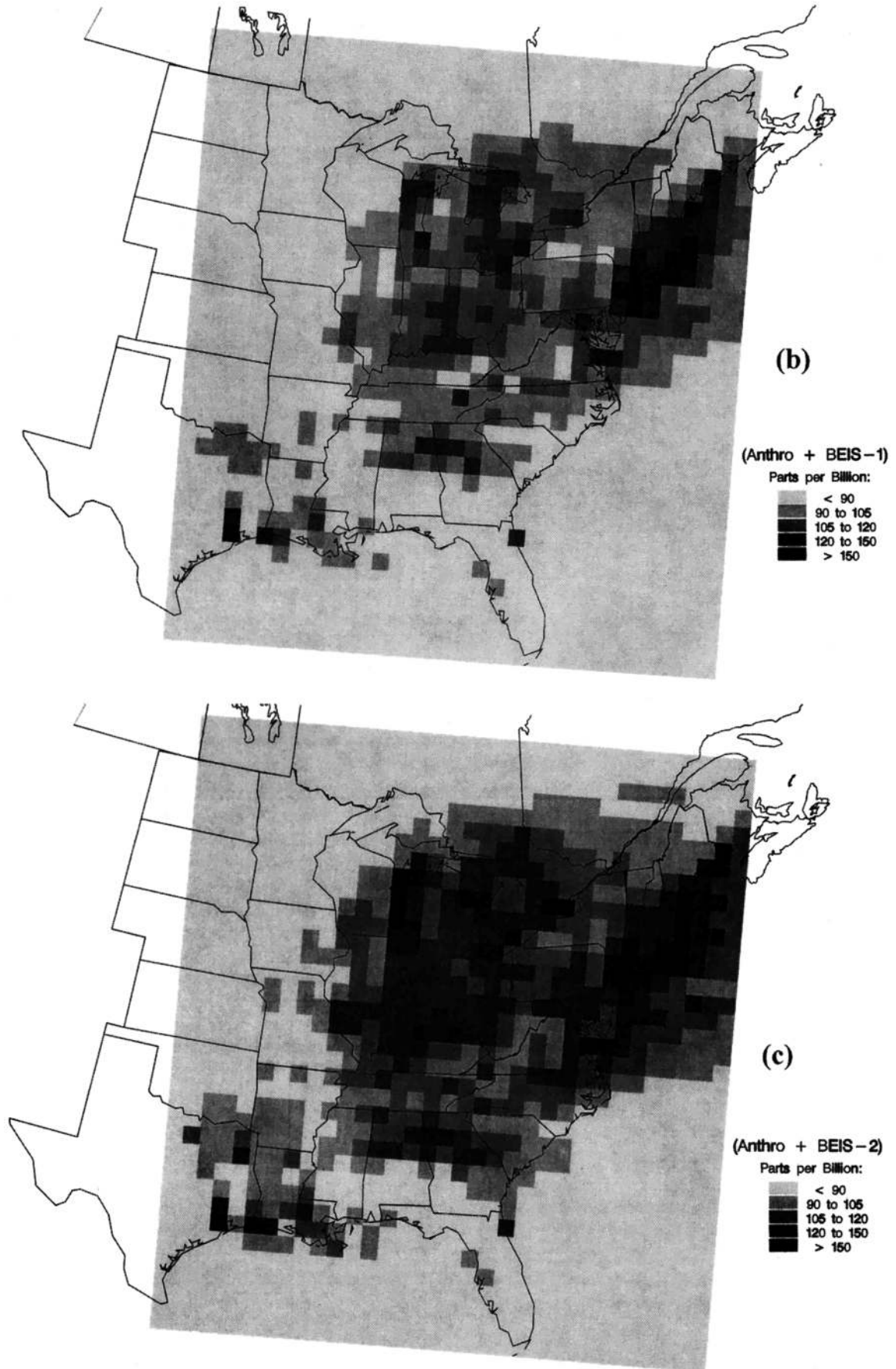


Figure 4. (continued)

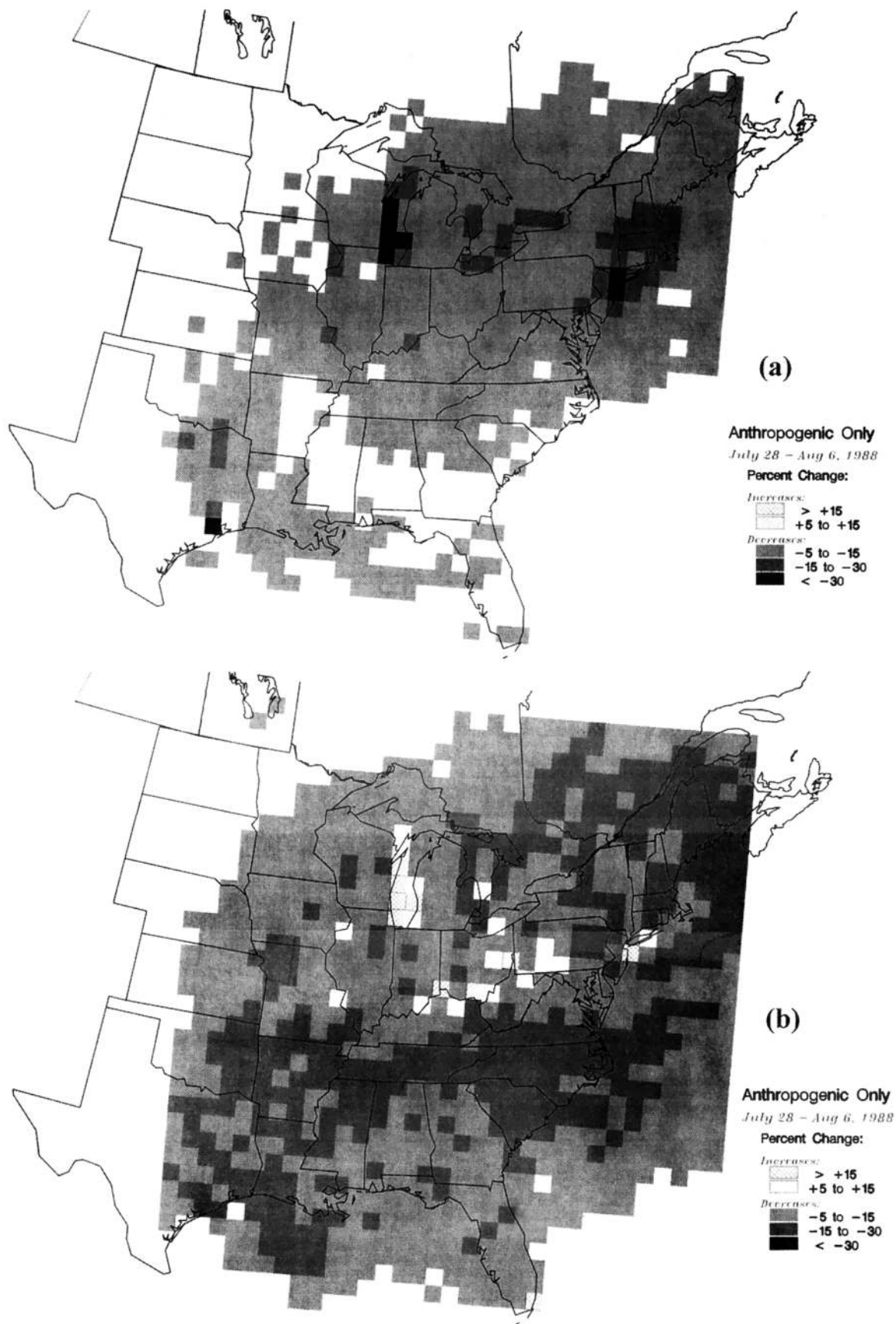


Figure 5. Percent change in maximum hourly ozone simulated with RADM as a function of biogenic emissions and anthropogenic emissions reduction scenario. (a) No biogenic emissions, 50% VOC reduction; (b) no biogenic emissions, 50% NO_x reduction; (c) BEIS1-equivalent emissions, 50% VOC reduction; (d) BEIS1-equivalent emissions, 50% NO_x reduction; (e) BEIS2, 50% VOC reduction; and (f) BEIS2, 50% NO_x reduction.

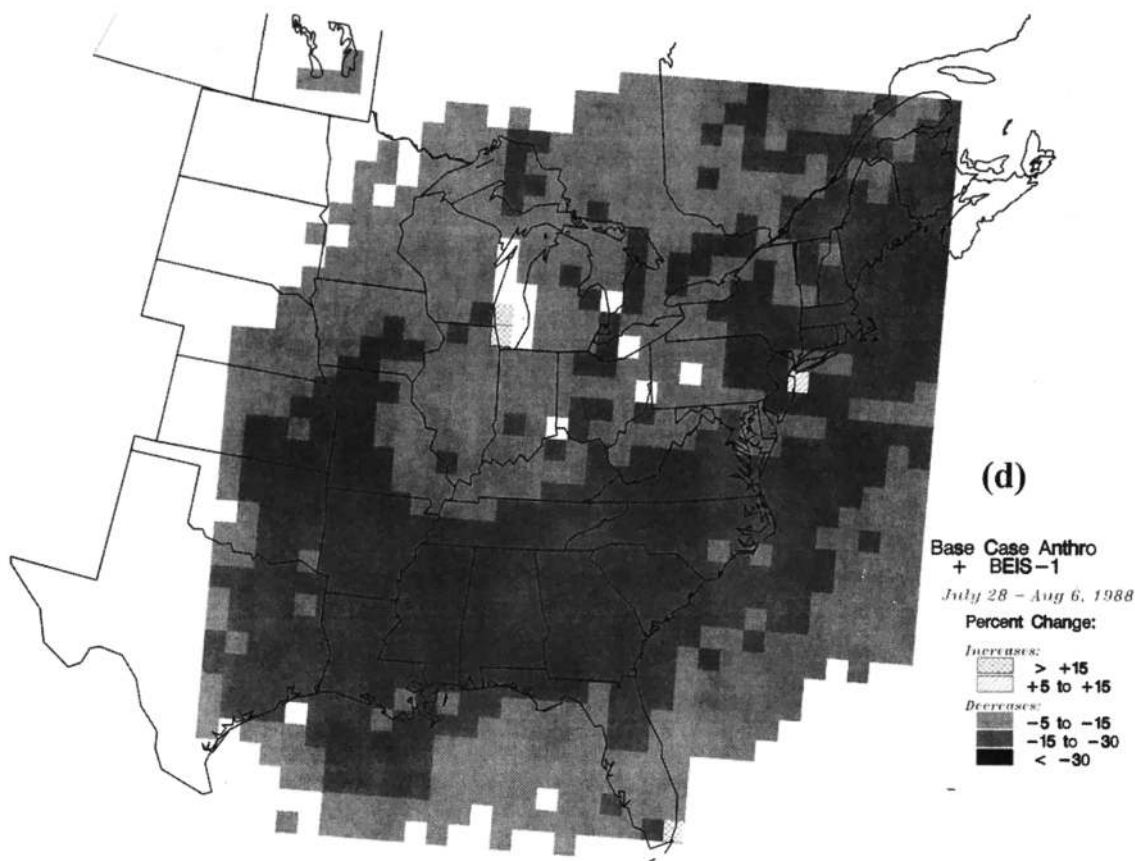
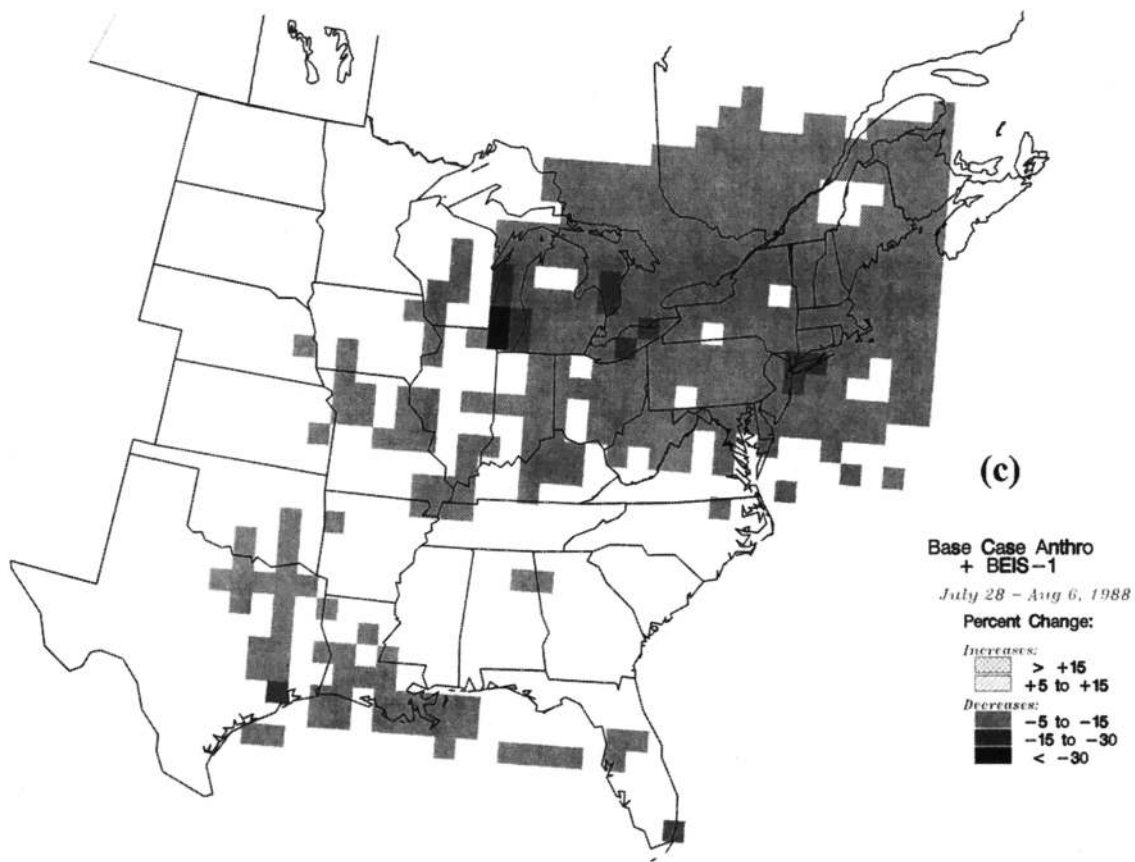


Figure 5. (continued)

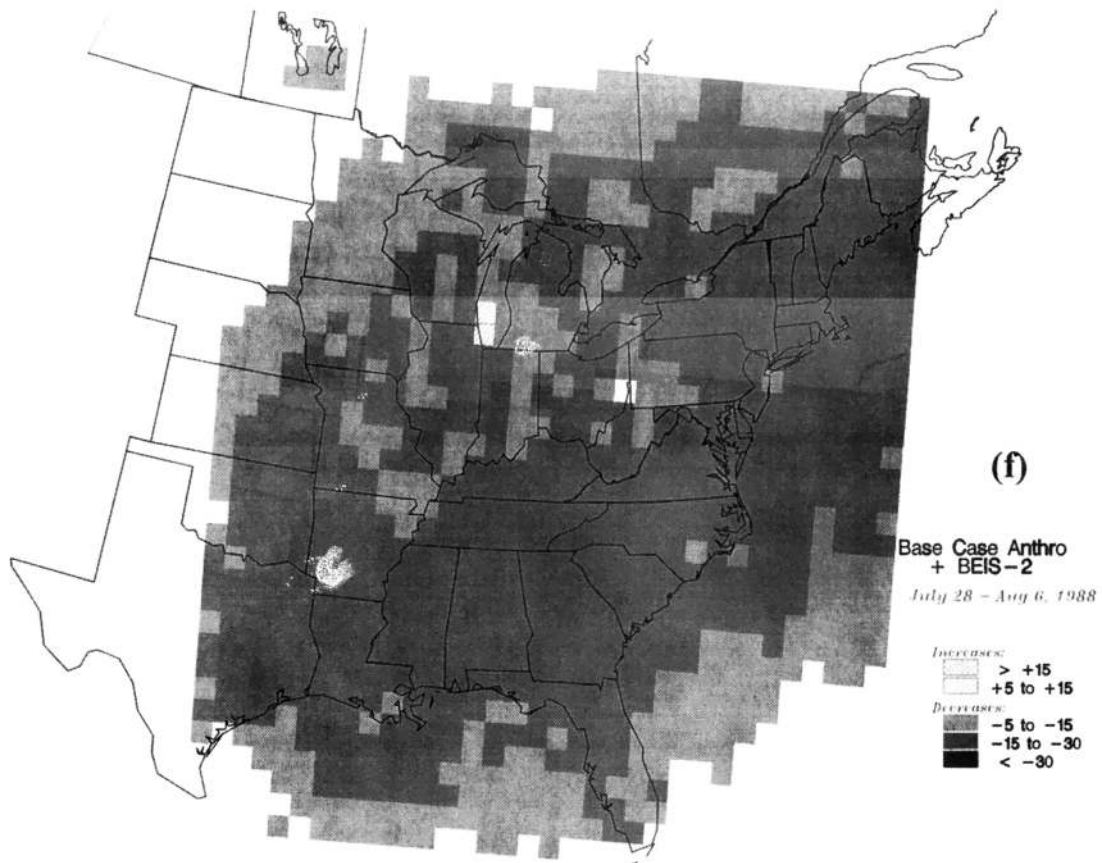
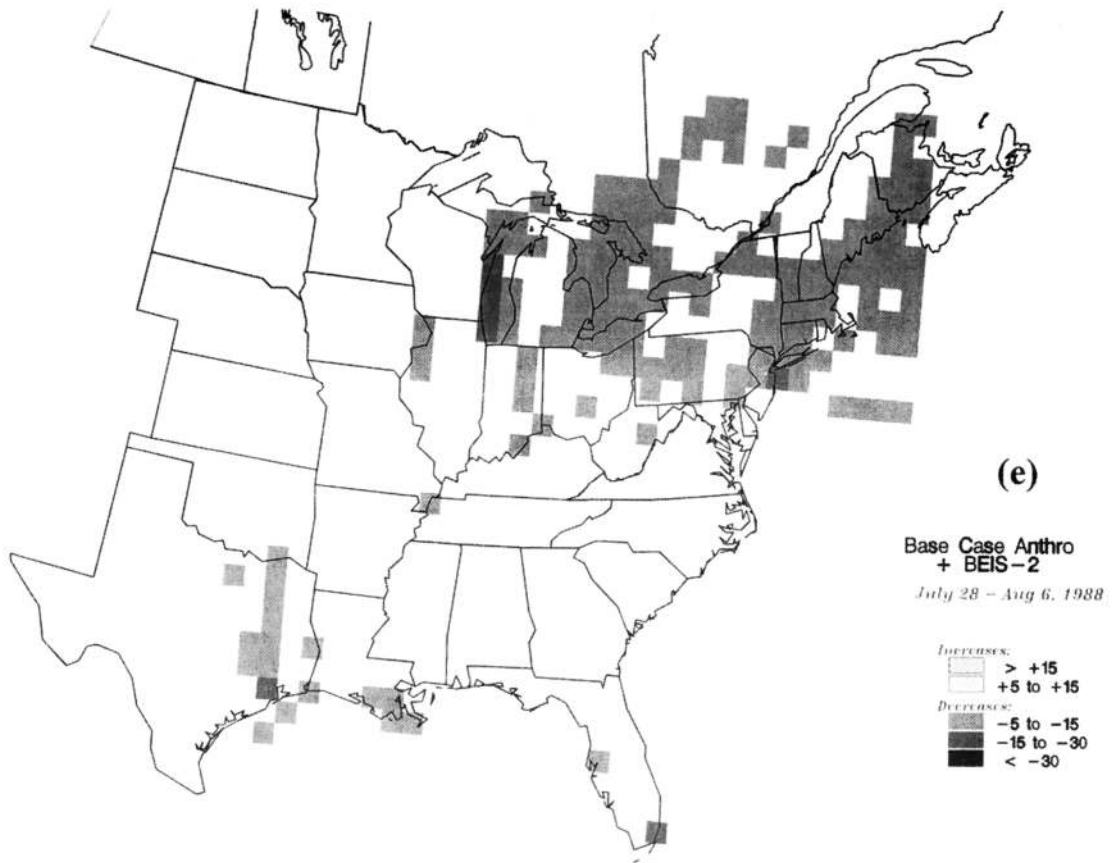


Figure 5. (continued)

Table 5. Sensitivity of Modeled Regional Ozone as a Function of Anthropogenic Emissions and Biogenic Emissions

Metric	Base			50% NO _x			50% VOC		
	No BEIS	BEIS1	BEIS2	No BEIS	BEIS1	BEIS2	No BEIS	BEIS1	BEIS2
Grid hours >80 ppb	6,326	17,271	28,073	2,380	6,397	11,896	2,371	12,475	24,841
Grid hours >120 ppb	150	743	2,306	82	279	573	2	189	1,459
Grid hours >150 ppb	0	44	290	0	21	76	0	1	129
Peak O ₃ , ppb (Column,row)	148 (31,27)	171 (31,27)	207 (15,26)	140 (15,26)	159 (15,26)	189 (15,26)	120 (31,29)	151 (31,27)	188 (15,26)

Modeled results from the RADM for July 28 to August 6, 1988, excluding results from 22 "urban" grid cells. Grid cell (1,1) is positioned at the southwest corner of the domain.

and the regional extent of elevated levels are increased with a change from BEIS1 to BEIS2. Second, the relative effectiveness of VOC versus NO_x control is shifted toward NO_x control with a change from BEIS1 to BEIS2.

4. Measured Versus Modeled Isoprene

4.1. Isoprene Measurements

Measured isoprene concentrations are obtained from an intensive field study conducted near Scotia, Pennsylvania, during July and August 1988. Most of the near-surface measurements were collected at 5 m above ground level in a ~3 ha clearing surrounded by an oak-dominated deciduous forest to the north, east, and south, and a pine-dominated forest to the west. During the Scotia study, approximately 150 30-min samples were analyzed via gas chromatography. *Martin et al.* [1991] provide additional details on the near-surface measurement program.

The limited number of upper air measurements included four vertical profiles from a 15 m tower situated in a nearby scrub oak forest, twenty-four tethered balloon profiles up to 100 m, and two aircraft "fly-overs" at heights extending to 1600 m. These measurement systems are briefly discussed by *Westberg et al.* [1991]. Additional description of the balloon

profiles is given by J. Greenberg et al. (Tethered balloon measurements of biogenic VOCs in the atmosphere, submitted to *Atmospheric Environment*, 1998). All of the upper air measurements and most of the near-surface measurements were made during the daylight hours.

4.2. Comparison of Measured and Modeled Isoprene

Isoprene concentrations from the RADM have been extracted from the grid cell and model layer(s) corresponding to the measured concentrations. As noted in Table 4, the grid cell overlaying Scotia is comprised of 73% forest and 33% oak crown cover, reflecting forest inventory data collected in this area [*Hansen et al.*, 1992]. Emissions computed for this grid cell are indicative of the rural character of the Scotia site and as noted in Table 7 are dominated by biogenic VOC emissions and relatively small emissions of anthropogenic and biogenic NO_x.

Table 8 compares measured isoprene concentrations with two sets of RADM base case simulations. The comparison consists of three vertical groupings: (1) a near-surface group consisting of 150 5-m measurements and concentrations from the first model layer; (2) a 100-m profile group consisting of available tower and tethered balloon measurements and concentrations averaged from model layers 1-3; and (3) a 1600-m profile group consisting of available tower, balloon, and aircraft measurements and concentration profiles averaged from model layers 1-13. Concentrations from layer one of RADM/BEIS2 average 25% less than the measured 5-m concentrations (4.5 ppbv versus 6.0 ppbv), while concentrations from RADM/BEIS1 are an order of magnitude smaller (0.6 ppbv). For both the 100 and 1600 m average profiles, RADM/BEIS2 concentrations are about 50% lower than that measured. RADM/BEIS1 concentrations are more than an order of magnitude lower than that measured. Profiles of isoprene obtained for the two periods when aircraft data were

Table 6. Relative Effectiveness of 50% VOC Anthropogenic Emission Reductions Versus 50% NO_x Anthropogenic Emissions on Modeled Regional Ozone as a Function of Biogenic Emissions

Ozone metric	No BEIS emissions	BEIS1 emissions	BEIS2 emissions
Number of grid hours >80 ppb	+0.1%	-35%	-46%
Number of grid hours >120 ppb	+53%	+12%	-38%
Number of grid hours >150 ppb	N.A.	+45%	-18%

Simulations based on the Regional Acid Deposition Model (RADM) for July 28 to August 6, 1988, excluding 22 "urban" grid cells. "N.A." means that there are no modeled grid cells >150 ppb. A shift between VOC and NO_x effectiveness is evident; positive values indicate that 50% VOC emissions are more effective, and negative values indicate that 50% NO_x emissions are more effective.

Table 7. Biogenic (BEIS1 and BEIS2) and Anthropogenic Emissions Estimated for the Scotia Grid Cell (24,24) Averaged Over the Period July 19-23, 1988

	Isoprene, kg C km ⁻² h ⁻¹	VOC, kg C km ⁻² h ⁻¹	NO _x , kg N km ⁻² h ⁻¹
BEIS1	0.6	1.6	0.01
BEIS2	3.0	4.0	0.01
Anthropogenic	-	0.6	0.06

Table 8. Summary of Observed and Modeled Isoprene at Scotia, Pennsylvania, for the Period July 22 to August 18, 1988

	Number of Values	Observed	RADM/BEIS1	RADM/BEIS2
Near surface	150	6.0 ± 3.1	0.6 ± 0.3	4.5 ± 2.2
100 m profiles	24	2.8 ± 1.0	0.2 ± 0.1	1.4 ± 0.4
1600 m profiles	2	1.3 ± 0.3	0.1 ± 0.05	0.7 ± 0.3

Values indicate the mean and the standard deviation. Units are ppbv.

available are shown in Figure 6. It is evident that, although RADM/BEIS2 shows a tendency to underpredict, it clearly performs better than RADM/BEIS1.

The average diurnal plot of observed and modeled near-surface concentrations is shown in Figure 7. Each binned point represents the mean (time and concentration) of 10 values. The binned points appear closer together during the daylight hours because of the higher frequency of measurements. For the daylight hours, RADM/BEIS2 is consistently about a factor of 2 lower than the measurements. Both modeled and observed concentrations peak around sunset, but observed values decrease much more rapidly than modeled values. Concentrations with RADM/BEIS1 are consistently lower than those measured except just before sunrise, when observed values reach a minimum.

To probe the processes responsible for the modeled diurnal behavior, we have extracted information from the RADM/BEIS2 simulation for July 31 to August 1, 1988, a period with a high frequency of observations. Figure 8 shows the observed and modeled isoprene concentrations, which behave similar to the mean diurnal plot in Figure 7. The processes from RADM model layer one contributing to isoprene production and destruction are plotted in Figure 9. The dominant processes in layer one are emissions (source) and vertical diffusion (sink). Although chemical reactions in layer one are important, they are nearly an order of magnitude less than vertical diffusion. The OH plus isoprene reaction contribution peaks near midday, while isoprene destruction from the O₃ and NO₃ reactions exceed that from the OH reaction beginning around sunset. The net production curve shows that competing processes nearly offset each other during much of the day, but the net production rate increases rapidly to 10 ppbv/h just before sunset (2300 UT). During this hour, vertical diffusion is only about a half (-17 ppbv/h) as large as emissions (+31 ppbv/h). Chemical destruction only removes about 4 ppbv/h. After the large peak in isoprene production, the only significant processes reducing isoprene at night are the O₃ and NO₃ reactions, which remove 1-2 ppbv/h.

This analysis suggests that modeled isoprene concentrations in layer one are very sensitive to the delicate balance of isoprene emissions (which are driven by solar radiation) and vertical diffusion (which is driven by sensible heat flux during the daytime). At night, the modeled isoprene concentrations appear to be affected mainly by a combination of vertical model resolution and the modeling of the stable boundary layer because the concentration time series is relatively insensitive to known uncertainties in the nighttime chemistry.

5. Discussion

Concern about the significant increase in isoprene emission estimates is understandable when viewed from a historical perspective. After a period of speculation during the 1970s, biogenic hydrocarbon emissions were dismissed as being unimportant to urban ozone formation [Altshuller, 1983; Lurmann *et al.*, 1984]. The issue was reexamined in the 1980s by Trainer *et al.* [1987] and Chameides *et al.* [1988] who pointed out that biogenic VOC emissions were probably important for ozone formation in rural areas and for affecting VOC/NO_x sensitivity near some urban areas. Meanwhile, a national biogenic emission inventory emerged for ozone modeling yielding VOC emissions on the same order of magnitude as anthropogenic emissions [Lamb *et al.*, 1993]. This inventory was quickly superceded by a methodology yielding even higher isoprene estimates [Geron *et al.*, 1994], which formed the primary basis of BEIS2. As the biogenic emission inventories were rapidly changing, ozone modelers in the air quality modeling community were grappling with the new challenge of predicting regional as well as urban ozone. The complexities associated with the move to regional models were increased by the large uncertainties with the biogenic emission estimates. To date, only a few studies [Roselle, 1994; Chock *et al.*, 1995; Sillman *et al.*, 1995; Jackson *et al.*, 1996; Morris *et al.*, 1997] have begun to piece together the impact of the higher isoprene emissions on modeled isoprene concentrations, ozone formation, and VOC/NO_x sensitivity.

We have described the algorithm for BEIS2, which at the time of this study represented a contemporary approach for generating a biogenic emissions inventory. Although not presented in this paper, the underlying basis of BEIS2 for estimating isoprene fluxes from deciduous forests has been evaluated with several field studies [Fuentes *et al.*, 1995; Guenther *et al.*, 1996; Pier and McDuffie, 1997]. It can be inferred from these micrometeorological and whole-tree field studies that isoprene flux estimates are accurate to within about 50% and that estimates of emissions with BEIS2 are superior to BEIS1.

We have examined how the evolution in biogenic emission estimates can affect ozone predictions and have shown that these changes have a major influence on ozone predicted with the RADM model (Table 5). Changes in modeled elevated ozone levels are quite sensitive to VOC versus NO_x emission reductions. In addition, across much of the RADM modeling domain, elevated levels of ozone went from being VOC sensitive to NO_x sensitive with the increased levels of biogenic VOC emissions resulting from BEIS2 (Table 6). These results are similar to those of Roselle [1994] who used the Regional Oxidant Model (ROM), but because of the relatively coarse resolutions in both modeling studies, further examination of urban areas using models with finer grid resolutions is needed.

While field studies support the assertion that isoprene fluxes from BEIS2 are superior to BEIS1, only a scant amount of information has been published on modeled versus observed isoprene concentrations. Comparing near-surface observations of isoprene versus calculations from the Urban Airshed Model, Morris *et al.* [1997] suggest that estimates from BEIS2 are much too high. These suggestions contrast with the results reported here, which indicate that using BEIS2 in RADM resulted in mean near-surface isoprene predictions that were slightly lower (25%) than observed.

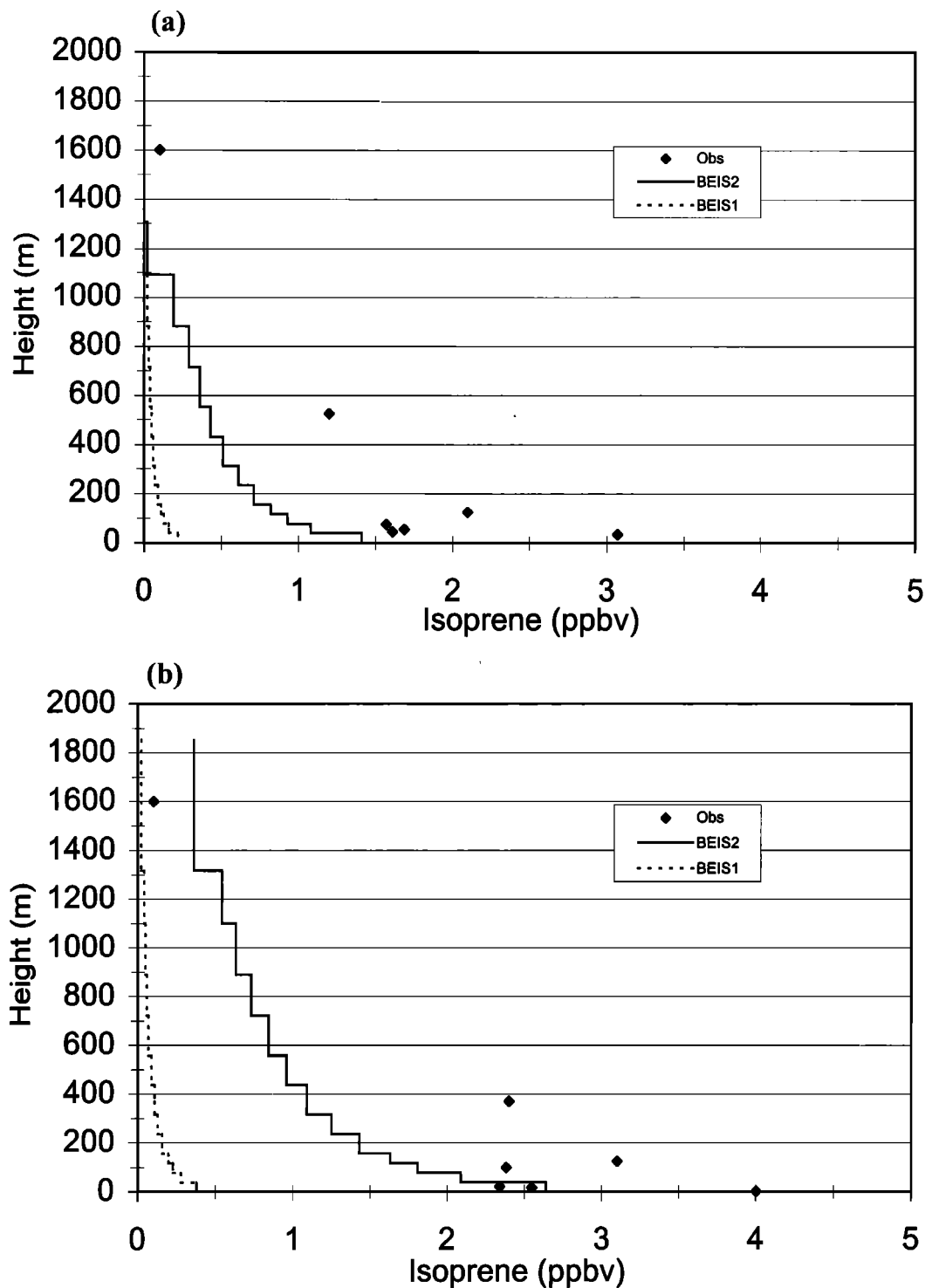


Figure 6. Vertical profiles of isoprene observed and modeled at Scotia, Pennsylvania: (a) 1100 LT, August 21, 1988 and (b) 1700 LT, August 22, 1988.

Although it can be instructive to examine near-surface isoprene concentrations, it is difficult to separate model shortcomings from measurement variability. In fact, *Andronache et al.* [1994] recommend that isoprene be measured well above the surface (starting about 40 m) because of the difficulties associated with analyzing isoprene measured near the surface, difficulties that can be attributed to rapid and spatially heterogeneous processes of emissions, vertical diffusion, and chemistry. Our analysis of daytime data collected above 40 m (Figures 6a-6b) indicated that BEIS2 resulted in

isoprene concentrations that are about 50% lower than observed values, with results from BEIS1 an order of magnitude too low. It is our judgement that the comparison of surface and upper air isoprene concentrations from the Scotia data set provides additional corroboration to the published field flux studies on the veracity of the BEIS2 isoprene estimates relative to BEIS1.

As shown in the diurnal plots (Figure 7), however, further improvement on the treatment of isoprene in regional ozone models such as the RADM is needed. In particular, the proc-

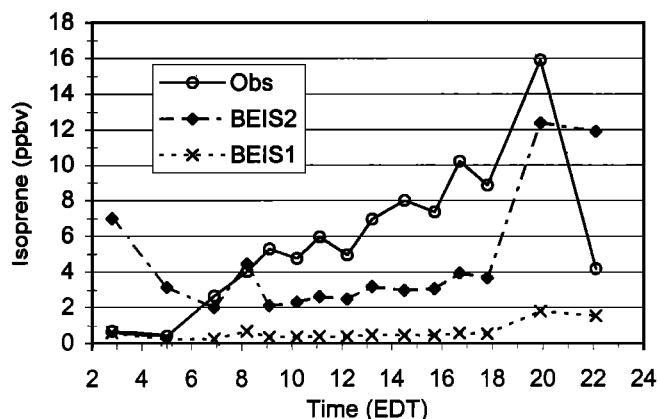


Figure 7. Mean diurnal plot of isoprene concentrations observed and modeled near the surface at Scotia, Pennsylvania, during July and August 1988. Data points represent the bin of 10 values.

ess analysis shown in Figures 9a-9b suggests that vertical diffusion should be handled carefully, particularly in the early morning and late afternoon hours. An area of possible improvement in the RADM would be to simulate vertical diffusion with emerging techniques such as transilient-turbulence theory [Inclan *et al.*, 1996]. Certainly, the vertical transport and diffusion of scalar substances emitted near the top of a forest canopy (which currently is poorly understood) should be examined under field conditions.

Another source of uncertainty in the modeling of isoprene is the possibility that deposition may provide a small but important sink of isoprene. *Cleveland and Yavitt* [1997] note that soils may remove as much as 5% of globally emitted isoprene on an annual basis. Currently, most air quality models assume negligible amounts of isoprene deposition.

While uncertainties exist with the photochemistry of isoprene and its reaction products, the primary destruction reactions with OH, NO₃, and O₃ are reliably known [Carter, 1996]. We further examined isoprene decay rates in sensitivity simulations with changes in NO₃ and N₂O₅ production and loss rates, and, although not shown in this paper, we found only minor impacts on the nighttime decay of isoprene. Thus the discrepancy in modeled and observed nighttime decay of isoprene probably is not caused by uncertainty in the isoprene chemistry, but it may result either from the air quality model's representation of horizontal advection, deposition, or vertical mixing or from the spatial variability of measured concentrations within the stable boundary layer.

Although uncertainty in the isoprene chemistry did not seem to cause the nighttime discrepancy we observed here, there is some uncertainty in the isoprene photochemistry of ozone production. It is important that future modeling studies include more complete descriptions of isoprene chemistry, like that proposed by Carter [1996]. Indeed, future evaluation studies would be well advised to examine longer-lived species associated with isoprene chemistry, such as methacrolein, methy vinyl ketone, and their PAN analogues. Unfortunately, most compressed photochemical mechanisms currently used

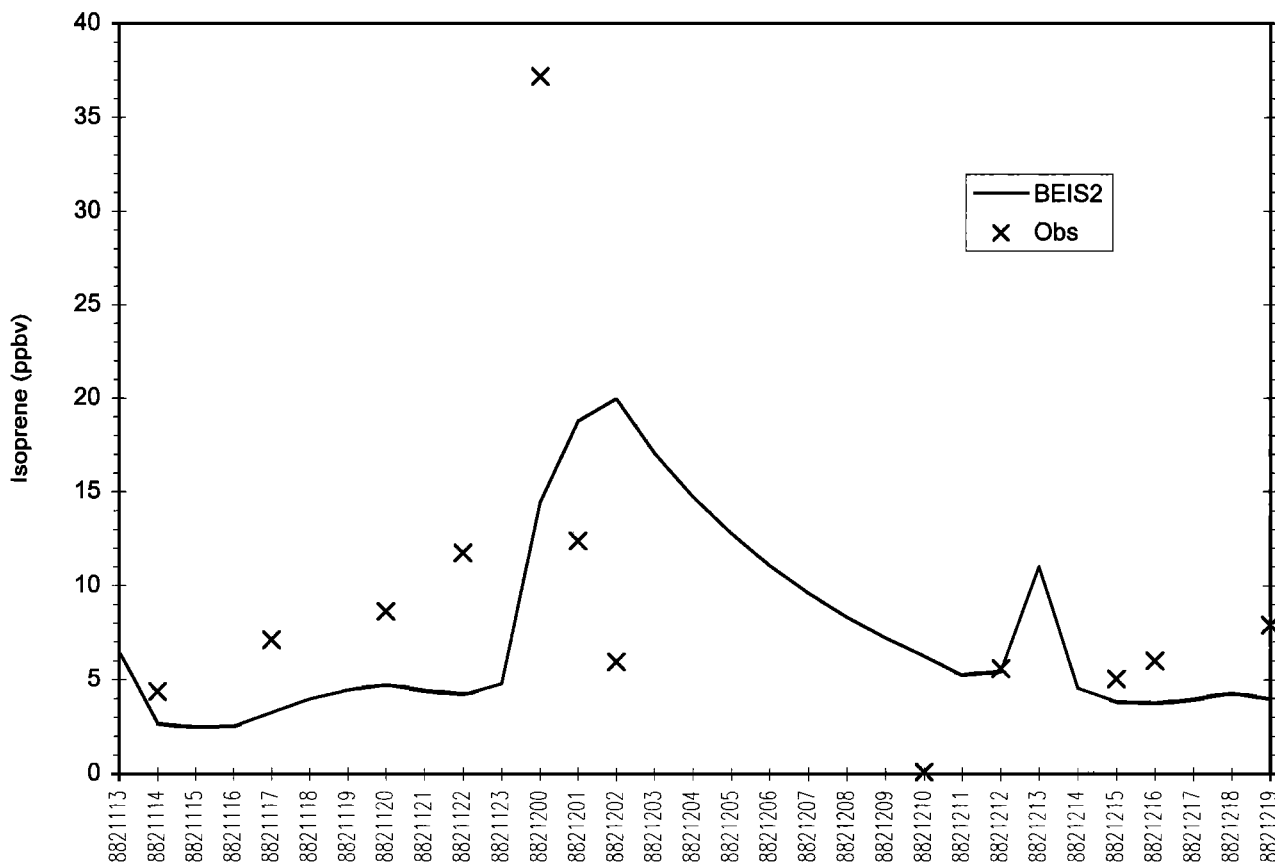


Figure 8. Diurnal plot of isoprene concentrations observed (near surface) and modeled (RADM layer 1) for Scotia, Pennsylvania, beginning at 1300 UT on July 31 and ending at 1900 UT on August 1, 1988.

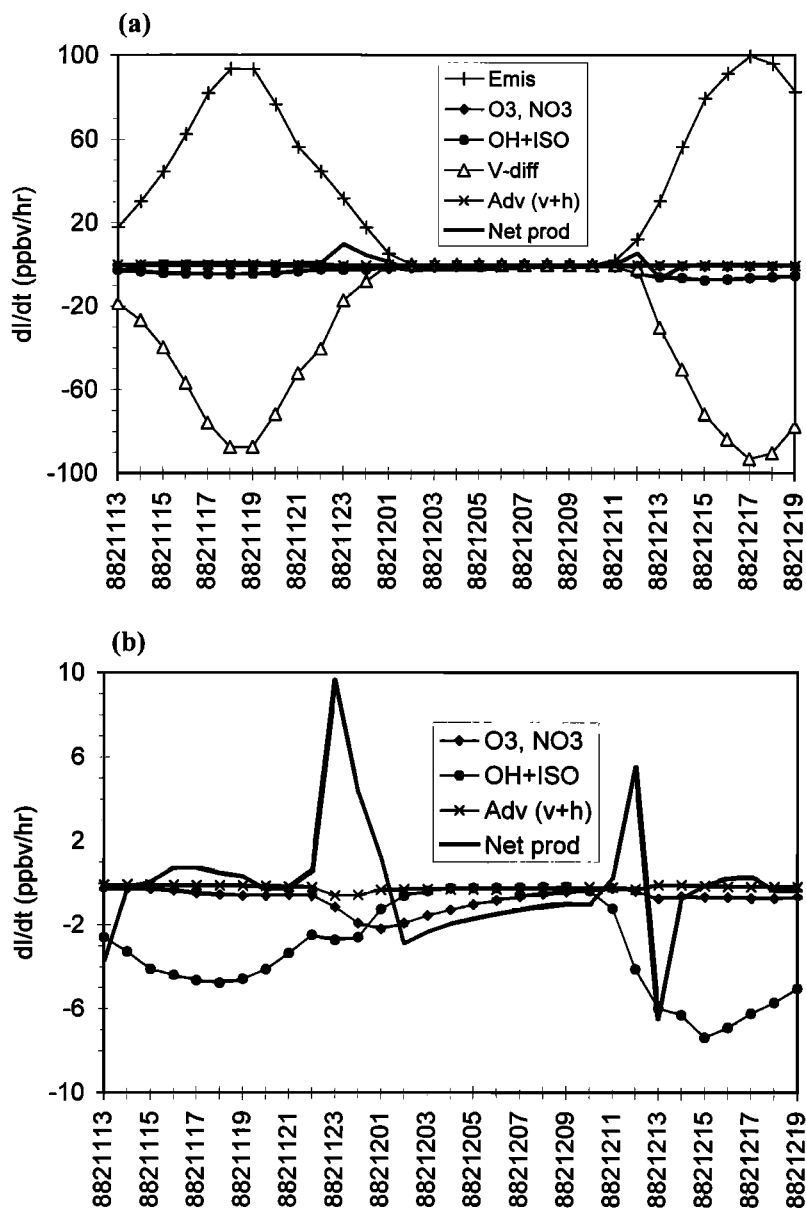


Figure 9. Diurnal plot of processes from RADM (layer 1) contributing to changes in isoprene (ppbv/h) for grid cell (24,24) beginning at 1300 UT on July 31, 1988 and ending at 1900 UT on August 1, 1988. (a) All major processes and net production and (b) chemistry, advection, and net production.

in air quality models, including RADM, do not represent these important decay products.

Because of the complexity involved with evaluating near-surface concentrations of isoprene, future studies would be advised to take an aggressive three-dimensional view, by examining extensive measurements of isoprene and its oxidation products throughout the first few hundred meters of the atmosphere and by examining horizontal variability. As we gain further understanding and make improvements in the chemical and physical processes in the models, work will undoubtedly continue on improving the accuracy of isoprene emission algorithms with upgrades in land use distributions, base emission factors, and environmental corrections.

Acknowledgments. The authors thank Jim Greenberg for providing vertical profiles of isoprene from the Scotia field study and are grateful to dedicated efforts of staff at DynTel Corporation who are

responsible for the day-to-day operation of the RADM model. Helpful comments and suggestions were provided by Shawn Roselle, Norm Possiel, and two anonymous reviewers. The information in this document has been funded in part by the U.S. Environmental Protection Agency. It has been subjected to Agency review and approved for publication. Mention of trade names or products does not constitute endorsement of use.

References

- Altshuller, P., Review: Natural volatile organic substances and their effect on air quality in the United States, *Atmos. Environ.*, **17**, 2131-2165, 1983.
- Andronache, C., W. Chameides, M. Rodgers, J. Martinez, P. Zimmerman, and J. Greenberg, Vertical distribution of isoprene in the lower boundary layer of the rural and urban southern United States, *J. Geophys. Res.*, **99**, 16,989-16,999, 1994.
- Byun, D., and R. Dennis, Design artifacts in Eulerian air quality models: Evaluation of the effects of layer thickness and vertical profile correction on surface ozone concentrations, *Atmos. Environ.*, **29**, 105-126, 1995.

- Carter, W., Condensed atmospheric photooxidation mechanism for isoprene, *Atmos. Environ.*, *30*, 4275-4290, 1996.
- Chameides, W., R. Linsay, R. Richardson, and C. Kiang, The role of biogenic hydrocarbons in urban photochemical smog: Atlanta as a case study, *Science*, *241*, 1473-1475, 1988.
- Chang, J., R. Brost, I. Asaksen, S. Madronich, P. Middleton, W. Stockwell, and C. Walchek, A three-dimensional Eulerian acid deposition model: Physical concepts and formulation, *J. Geophys. Res.*, *92*, 14,681-14,700, 1987.
- Chock, D., G. Yarwood, A. Dunker, R. Morris, A. Pollack, and C. Schleyer, Sensitivity of Urban Airshed Model results for test fuels to uncertainties in light-duty vehicle and biogenic emissions and alternative chemical mechanisms - Auto/Oil Air Quality Improvement Research Program, *Atmos. Environ.*, *29*, 3067-3084, 1995.
- Cleveland, C., and J. Yavitt, Consumption of atmospheric isoprene in soil, *Geophys. Res. Lett.*, *24*, 2379-2382, 1997.
- Dennis, R., W. Barchet, T. Clark, and S. Seilkop, Evaluation of regional acidic deposition models (part 1), in *National Acid Precipitation Assessment Program: State of Science and Technology*, Vol. 1, *NAPAP SOST Rep. 5*, Natl. Acid Precip. Assess. Program, Washington, D. C., 1990.
- Dimitriades, B., and A. Altshuller, International conference on oxidant problems: Analysis of the evidence/viewpoints presented, 1, Definition of key issues, *J. Air Pollut. Control Assoc.*, *27*, 299-307, 1977.
- Fuentes, J., D. Wang, G. Hartog, H. Neumann, T. Dann, and K. Puckett, Modelled and field measurements of biogenic hydrocarbon emissions from a Canadian deciduous forest, *Atmos. Environ.*, *29*, 3003-3017, 1995.
- Geron, C., A. Guenther, and T. Pierce, An improved model for estimating emissions of volatile organic compounds from forests in the eastern United States, *J. Geophys. Res.*, *99*, 12,773-12,791, 1994.
- Geron, C., T. Pierce, and A. Guenther, Reassessment of biogenic volatile organic compound emissions in the Atlanta area, *Atmos. Environ.*, *29*, 1569-1578, 1995.
- Grell, G., J. Dudhia, and D. Stauffer, A description of the fifth-generation Penn State/NCAR mesoscale model (MM5), *NCAR/TN-398+STR*, 138 pp., Natl. Cent. for Atmos. Res., Boulder, Colo., 1994.
- Guenther, A., P. Zimmerman, and M. Wildermuth, Natural volatile organic compound emission rate estimates for U.S. woodland landscapes, *Atmos. Environ.*, *28*, 1197-1210, 1994.
- Guenther, A., et al., A global model of natural volatile organic compound emissions, *J. Geophys. Res.*, *100*, 8873-8892, 1995.
- Guenther, A., P. Zimmerman, L. Klinger, J. Greenberg, C. Ennis, K. Davis, W. Pollock, H. Westberg, G. Allwine, and C. Geron, Estimates of regional natural volatile organic compound fluxes from enclosure and ambient measurements, *J. Geophys. Res.*, *101*, 1345-1359, 1996.
- Hansen, M., T. Frieswyck, J. Glover, and J. Kelly, *The Eastwide Forest Inventory Database: User's Manual*, U.S. For. Serv., *Dep of Agric. Gen. Tech. Rep. NC-151*, 1992.
- Inclan, M., R. Forkel, R. Dlugi, and R. Stull, Application of transilient turbulent theory to study interactions between the atmospheric boundary layer and forest canopies, *Boundary Layer Meteorol.*, *79*, 315-344, 1996.
- Jackson, B., E. Mulberg, and N. Wheeler, The application of biogenic emission inventory estimates to photochemical modeling in California, paper presented at the 9th AMS/ AWMA Joint Conference on Applications of Air Pollution Meteorology, Atlanta, Ga., Jan. 28 to Feb. 25, 1996.
- Kinnee, E., C. Geron, and T. Pierce, United States land use inventory for estimating ozone precursor emissions, *Ecol. Appl.*, *7*, 46-58, 1997.
- Lamb, B., D. Gay, H. Westberg, and T. Pierce, A biogenic hydrocarbon emission inventory for the U.S.A. using a simple canopy model, *Atmos. Environ., Part A*, *27*, 1673-1690, 1993.
- Lamb, B., T. Pierce, D. Baldocchi, E. Allwine, S. Dilts, H. Westberg, C. Geron, A. Guenther, L. Klinger, P. Harley, and P. Zimmerman, Evaluation of forest canopy models for estimating isoprene emissions, *J. Geophys. Res.*, *101*, 22,787-22,797, 1996.
- Lurmann, F., B. Nitta, K. Ganeson, and A. Lloyd, Modeling potential ozone impacts from natural hydrocarbons, III, Ozone modeling in Tampa/St. Petersburg, Florida, *Atmos. Environ.*, *18*, 1133-1143, 1984.
- Martin, R., H. Westberg, E. Allwine, L. Ashman, J. Farmer, and B. Lamb, Measurement of isoprene and its atmospheric oxidation products in a central Pennsylvania deciduous forest, *J. Atmos. Chem.*, *13*, 1-32, 1991.
- Morris, R., K. Lee, and G. Yarwood, Phase I comparison of OTAG UAM-V/BEIS2 results with ambient isoprene and other related species concentrations, technical report, 22 pp., Am. Automobile Manuf. Assoc., Detroit, Mi., 1997.
- National Research Council, *Rethinking the Ozone Problem in Urban and Regional Air Pollution*, 489 pp., Natl. Acad. Press, Washington, D. C., 1991.
- Nowak, D., R. Rowntree, G. McPherson, S. Sisinni, E. Kerkmann, and J. Stevens, Measuring and analyzing urban tree cover, *Landsc. Urban Plan.*, *36*, 49-57, 1996.
- Pier, P., and C. McDuffie, Seasonal isoprene emission rates and model comparisons using whole-tree emissions from white oak, *J. Geophys. Res.*, *102*, 23,963-23,971, 1997.
- Pierce, T., and P. Waldruff, PC-BEIS: A personal computer version of the Biogenic Emissions Inventory System, *J. Air Waste Manage. Assoc.*, *41*, 937-941, 1991.
- Pierce, T., B. Lamb, and A. Van Meter, Development of a biogenic emissions inventory system for regional air pollution models, paper presented at Annual Meeting of the Air & Waste Management Association, Pittsburgh, Pa., 1990.
- Roselle, S., Effects of biogenic emission uncertainties on regional photochemical modeling of control strategies, *Atmos. Environ.*, *28*, 1757-1772, 1994.
- Sharkey, T., P. Vanderveer, and F. Loreto, Biogenic hydrocarbons: Measurements on corn and kudzu in 1992, paper presented at the AWMA Conference on Emission Inventory Issues in the 1990s, Durham, N. C., 1992.
- Sillman, S., et al., Photochemistry of ozone formation in Atlanta, GA - Model and measurements, *Atmos. Environ.*, *29*, 3055-3066, 1995.
- Sillman, S., D. He, C. Cardelino, and R. Imhoff, The use of photochemical indicators to evaluate ozone-NO_x-hydrocarbon sensitivity: Case studies from Atlanta, New York, and Los Angeles, *J. Air Waste Manage. Assoc.*, *47*, 1030-1040, 1997.
- Simpson, D., Biogenic emissions in Europe, 2, Implications for ozone control strategies, *J. Geophys. Res.*, *100*, 22,891-22,906, 1995.
- Stockwell, W., P. Middleton, J. Chang, and X. Tang, The second generation regional acid deposition model chemical mechanism for regional air quality modeling, *J. Geophys. Res.*, *95*, 16,343-16,376, 1990.
- Trainer, M., E. Williams, D. Parrish, M. Buhr, E. Allwine, H. Westberg, and F. Fehsenfeld, Models and observations of the impact of natural hydrocarbons on rural ozone, *Nature*, *329*, 705-707, 1987.
- U.S. Environmental Protection Agency, Regional interim emission inventories (1987-1991), vol. 1, Development methodologies, *EPA-454/R-93-021a*, Off. Air Qual. Plann. and Stand., Research Triangle Park, N. C., 1993.
- Wesely, M., Parameterization of surface resistances to gaseous dry deposition in regional-scale numerical models, *Atmos. Environ.*, *23*, 1293-1304, 1989.
- Westberg, H., B. Lamb, R. Martin, E. Allwine, P. Goldan, W. Kuster, P. Zimmerman, J. Greenberg, R. Seila, and W. Lonneman, Spatial and temporal behavior of isoprene in a deciduous forested region, paper presented at the CHEMRAWN VII World Conference on the Chemistry of the Atmosphere: Its Impact on Global Change, Baltimore, Md., Dec. 2-6, 1991.
- Williams, E., A. Guenther, and F. Fehsenfeld, An inventory of nitric oxide emissions from soils in the United States, *J. Geophys. Res.*, *97*, 7511-7519, 1992.
- Zimmerman, P., Determination of emission rates of hydrocarbons from indigenous species of vegetation in the Tampa/St. Petersburg, Florida Area, *EPA-904/9-77-028*, U.S. Environ. Prot. Agency, Atlanta, Ga., 1979.

L. Bender, DynTel Corp., PO Box 12804, RTP, NC 27709.
 R. Dennis, T. Pierce (corresponding author), and G. Tonnesen, USEPA, MD-80, RTP, NC 27711. (email: pierce.tom@epa.gov)
 C. Geron, USEPA, MD-62, RTP, NC 27711.
 A. Guenther, NCAR, PO Box 3000, Boulder, CO 80307.

(Received December 8, 1997; revised April 9, 1998; accepted May 21, 1998.)